UNIVERSITÀ
DI TORINO

Università degli Studi di Torino

Corso di laurea magistrale Interateneo
in Fisica dei sistemi complessi

Sensitivity analysis of climate change risk assessment

Master of Science thesis

Supervisor
Prof. Elisa Palazzi

Co-supervisor
Dr. Jacopo Grassi

Candidate
Marco Casari

Academic Year 2023/2024

Acknowledgements

My gratitude goes to Prof. Elisa Palazzi for her kindness and professionalism, Dr. Jacopo Grassi for his help and patience, having teached me the basics of topics this project is based on, and WSP Italia S.r.l., for the opportunity to develop the project in a company and the resources they provided. In particular I refer to Dr. Roberto Mezzalama, who accepted my request and shared ideas with enthusiasm, and to Dr. Massimo Dragan and his team, for the friendly hospitality during the months of work.

[35] was downloaded from the Copernicus Climate Change Service (2024). The results contain modified Copernicus Climate Change Service information 2024. Neither the European Commission nor ECMWF is responsible for any use that may be made of the Copernicus information or data it contains.

Climate scenarios used were from the NEX-GDDP-CMIP6 dataset, prepared by the Climate Analytics Group and NASA Ames Research Center using the NASA Earth Exchange and distributed by the NASA Center for Climate Simulation (NCCS).

Contents

Chapter 1

Introduction

1.1 Conceptual overview

Climate change is shaping ecosystems and human activities and is becoming a central topic of discussion across all fields [40, 50]. Effects of climate change have different severity, often changing with time and with the evolution of contexts they occur [26]. These impacts may depend also on the spatial scale of the systems affected [21].

The knowledge of present and future impacts of climate change becomes essential to reduce adverse outcomes, as well as to leverage potential benefits. Even more relevant is the concept of risk which moves the focus from the impacts to their potential occurrence, broadening the possibilities for related studies and actions. In fact, an increasing number of organisations are incorporating climate change risk assessments (CCRAs) into their decision processes [13]. A definition of risk assessment is given by Intergovernmental Panel on Climate Change (IPCC) as *the qualitative and/or quantitative scientific estimation of risks*, from [44, p. 2246], and CCRA is its restriction to climate-related risks.[1] Other authorities employ similar definitions of risk assessment and remark its usefulness [41, 63].

More generally, a risk assessment is essential part of the process of risk management, which uses the assessed information to reduce risk through the application of, e.g. policies, strategies, adaptation plans [5]. The objectives of risk management are defined in the broad field of disaster risk reduction (DRR) [55].

CCRA combines DRR practices and concepts with climate information [30, 29]. Some insights on the synergy between the fields of DRR and climate change adaptation are exposed in [29, pp. 469–471].

Credible climate information are refined by scientific data and in cooper-

[1] Terms *climate change risk assessment* and *climate risk assessment* are used equivalently in literature (cf. [30, p. 11] and [59, p. 20], also [43]). In this document the former is used, to highlight the focus on risks arising from climate change.

ation with users and stakeholders. They are the product of climate services, being the provision of climate-related data and information to assist decision-making [37]. An overview of the evolving field of climate services is available in [21, pp. 1431–1433] and in [52, pp. 1862–1869].

Various regulations, standards and guidelines for CCRA are available, but very few specify in detail the methodology to follow [43]. Methodologies differ by various means, e.g. the steps required to gather preliminar information on impacts and risks, the analysis of the system exposed, the evaluation of risk and its components, the presentation of outcomes (cf. [41, 26, 59, 10, 16], also see [43, pp. 10–11] and [30, p. 9]). This variety hinders the comparison of CCRA outcomes, diminishing their credibility and interoperability [33].

A single methodology may be chosen to perform the CCRA, but the issue presents once again since the methodology may not define operational details, e.g. functions and procedures involved. Implementation details are left to the authors of the CCRA, who base the choice on their experience and on scientific literature, according to the principles of climate services. To evaluate the dependence of risk on the functional representation of its components is the objective of this work.

The methodology of CCRA applied in the present work follows [59] and its upgrade [30]. The latter should be read in parallel with the former and supersedes outdated concepts.

1.1.1 Climate risk

Before stating the objective of the present study, first it is convenient to introduce a proper terminology. Definitions by International Organization for Standardization (ISO) are used for their concision. When some terms are not available, they are taken from IPCC. Both sources have similar definitions for the same terms.

Risk is a general term which can be tailored to different contexts and applications as a measure of uncertain consequences on a system of interest.[2] A system is very broadly any concrete or abstract entity which can be affected by risk.

Example

Some possible systems which can be exposed to risks are any physical system, communities of people, an idea.

A paradigmatic example is the financial sector, where the concept of risk is widely known and is connected directly to economic value and the concept

[2] Without delving into Philosophy, a source of change is needed to have consequences and it is specified by the definitions in use.

of portfolio, to the point that financial risk management can be considered a research field itself [15]. Examples on how other fields implement the concept are elaborated in [30, p. 14] and in [53].

In this work the risk related to climate change is: *effect of uncertainty*, from [41].[3] IPCC proposes a similar definition, expanding on the entities involved (e.g. the possible systems) and the contexts in which the term is used, but focusing only on negative effects: *the potential for adverse consequences for human or ecological systems, recognizing the diversity of values and objectives associated with such systems. In the context of climate change, risks can arise from potential impacts of climate change as well as human responses to climate change. Relevant adverse consequences include those on lives, livelihoods, health and well-being, economic, social and cultural assets and investments, infrastructure, services (including ecosystem services), ecosystems and species. [...]*, from [44, p. 2246]. An important aspect of climate risk is that it originates from both impact of climate change, i.e. *effect on natural and human systems (3.3)*, from [41], and any response to it, i.e. action enact to mitigate the effects of climate change or adapt to it. It is not common to see responses integrated into risk assessment, as exposed by [57, p. 492], and for the purposes of the present study they are neglected. From this perspective, two types of climate risk are studied in CCRAs: transition risk and physical risk. The former regards impacts on finance, economy and society caused by decarbonisation and transitioning to a sustainable economy, the latter is the risk related to the realisation of physical hazards. Both types of risk are assessed by organisations and financial institutions [14, 58]. Physical risks are further divided in acute and chronic, for extreme weather events and long term impacts, respectively [14, p. 10]. Henceforth, terms climate risk and risk are used interchangeably and both refer to climate-related physical risks.

To make the assessment easily extensible and modular, risk is defined as the result of the interaction of three elements, i.e. its determinants, namely hazard, exposure and vulnerability. Response is considered the fourth determinant of risk, when the adopted methodology includes it in the assessment. Definitions of determinants were introduced in [29, pp. 69–70] and offer a change of direction from previous methodologies centered on the concept of vulnerability of the system instead of the overall risk (cf. [59] and [30]).

The hazard is defined by ISO as *potential source of harm*, from [41] and is elaborated further by IPCC on which subjects it applies to. No particular reference is made to the climate system in the definitions, hence IPCC provides the more specific term climatic impact-driver (CID) in [44, p. 2224] to address to climate-related physical phenomena and with a neutral connotation (cf. [53, p. 10] or [52, pp. 1871–1872]). In the following the term

[3]Note that this definition is not specific to climate risk since no reference to climate is made.

hazard is used to address to climate-related hazards for brevity.

The exposure of a system is determined by *presence of people, livelihoods, species or ecosystems, environmental functions, services, resources, infrastructure, or economic, social or cultural assets in places and settings that could be affected*, from [41].

The vulnerability of a system is *propensity or predisposition to be adversely affected*, from [41]. Properties of the system which determine its vulnerability may be classified further in sensitivity, i.e. *degree to which a system (3.3) or species is affected, either adversely or beneficially, by climate (3.4) variability or change*, from [41], and adaptive capacity, i.e. *ability of systems (3.3), institutions, humans, and other organisms to adjust to potential damage, to take advantage of opportunities, or to respond to consequences*, from [41]. This classification in general helps the analysis of the system and the identification of responses, e.g. adaptation measures may increase the adaptive capacity of some elements of the system.

Each determinant may be viewed as a collection of elements, which are of different nature depending on the determinant they belong to, but are addressed generically as drivers.[4] CIDs with negative impacts are effectively drivers within the hazard determinant which are related to the climate system. Physical elements of the system may be effectively considered as drivers of exposure.[5]

Example

A tropical storm is a driver within the hazard determinant [30, p. 15], income is a driver within the vulnerability determinant [57, p. 493], airport structures (e.g. runways, aprons, terminals) in an airport (i.e. the system) are drivers within the exposure determinant [19, p. 551]. More examples are available in the references.

The concept of driver of risk is borrowed from [57] to allow a smooth extension to methodologies where risk is the result of complex interactions within and across determinants. In section 1.1.2 this topic is described further.

For a quantitative CCRA, numerical values must be associated to drivers. These values are called indicators and defined by ISO as: *quantitative, qualitative or binary variable that can be measured or described, in response to a defined criterion*, from [41].[6] There can be more than one way to describe

[4]When this terminology is not applied, it is common to refer to drivers with the name of the determinants they belong to, e.g. drivers within the vulnerability determinant are simply called vulnerabilities.

[5]In literature different terms are used to refer to drivers within the exposure, e.g. *assets* or *exposed sample* in [19].

[6]The definition by IPCC is not as general because focuses only on the climate system and there is no specific term for the same concept applied to the other determinants.

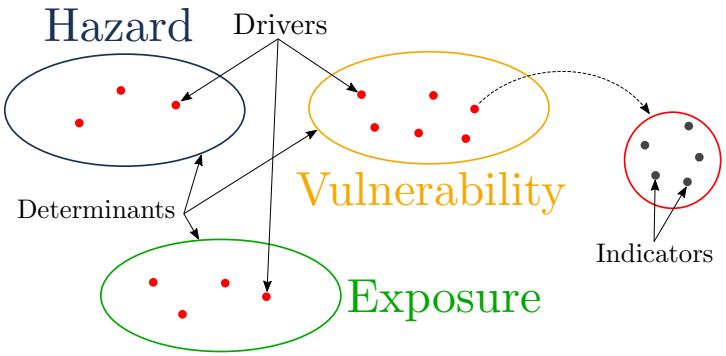

Figure 1.1: A possibile representation of the components of climate risk. Climate hazards can affect exposed and vulnerable elements of the system and determine a risk for it. Collectively these factors are called drivers and can grouped in the three independent determinants of risk: hazard, exposure and vulnerability. To provide quantitative results, each driver is described by numerical values, i.e. the indicators, each providing a different possible description or measure of the same driver.

numerically the same driver, hence the choice is not unique and the resulting risk may be affected by it.

Example

A drought is defined in general by IPCC as *an exceptional period of water shortage for existing ecosystems and the human population (due to low rainfall, high temperature, and/or wind)*, from [44, p. 2226]. Drought is a driver of risk and is a physical phenomena related to climate, hence it belongs to the hazard determinant.
Many indicators of drought are used, e.g. consecutive number of dry days, temperature, indicators combining temperature,precipitation and evotranspiration. See [29, pp. 167–169] for further examples and references; note that the term *index* is used in place of indicator.

In the following, the term indicator written alone refers to an indicator of a driver within the hazard determinant, to relax the lenghty wording. For the other determinants the full qualification is used.

Having introduced the definitions above, the various components of risk can be arranged as in figure 1.1. It sums up the relation between the various components, highlightning the fact that risk depends on drivers from three independent categories and are quantified possibly in multiple ways.

1.1.2 Complex risk

Unlike other types of risk assessment, e.g. probabilistic risk assessment, CCRA focuses on interactions between drivers instead of estimating their likelihood [30, pp. 20–21]. However, it is common to study each determinant

in isolation. Instead, an integrated risk assessment which is able to relate drivers within and across determinants would be able to describe the overall risk more accurately [7, pp. 145–147].

Interacting elements are not considered mainly because a proper formalisation of the interactions is difficult and rarely clear. In [57] the list of complex risk adopted by IPCC in Sixth Assessment Report (AR6) is extended, to allow more granularity in the assessment, and three categories of complex risk are proposed. The objective is to build a framework which helps to address to complex interactions more easily, thus helping their adoption in CCRAs. Response is included in the determinants, e.g. to introduce negative effects on vulnerability due to maladaptation. Depending on what is the origin of risk, the categories are:[57, p. 493]

1. interacting drivers within the same determinant;
2. interacting drivers across different determinants;
3. interacting risks.

In general, category 1 is considered as long as the methodology admits an aggregation of drivers to obtain each determinant.

Example

Flood risk in a geographical area is assessed. First, only artificial constructions are considered as system. The change in time of precipitation and temperature, i.e. drivers of risk within the hazard determinant, are aggregated to give a measure of the hazard. With this value and the analogous values of the other determinants, a category 1 risk can be evaluated, which measures the interaction of its determinants only defined by the methodology and lacking a particular meaning.
A collateral change in soil properties due to precipitation and temperature is added to the study. This results in a decrease of soil adaptive capacity, hence an increase of the vulnerability of buildings in that area. This interaction belongs to category 2.
A second iteration of the CCRA moves the focus to human activities in the area under study. When the corrispondent risk is evaluated, it can be merged with the risk value found previously to summarise the overall flood risk, which becomes a category 3 complex risk.

All three categories of complex risk may be found in the methodology (see section 2.3 for details), but in the present work only category 1 is considered, as there is no particular relation between drivers within different determinants, except for the aggregation into the final risk value. Nevertheless, extending the current study by introducing complexity throught the other categories may be interesting to test the robustness of the results.

From a mathematical point of view, complex interactions between drivers translate to mathematical functions which relate indicators. They may be treated as additional indicators to consider in the aggregation of determinants [48, pp. 39–40]. In the chosen methodology, no specific interaction is considered between drivers across determinants. This translates into linear relations between indicators when they are aggregated.

1.1.3 Problem statement

The objective of this work is to show how the risk evaluated following a given methodology depends on the choice of indicators. In particular, the study is restricted to indicators of hazard and their definitions are modified by varying the parameters they depend on.

Technically this study resembles a sensitivity analysis (SA): the effects on the outcome of a system by varying its input factors are assessed and attributed to specific input factors [20, pp. 627–632]. In this case the system is the CCRA and the methodology which implements it, its outcome is the risk value and the input factors are the parameters. More in detail, this work adopts a global approach to SA, since the space of all possible parameters, or a significative subset of it, is explored. This is essential for a significative SA, because indicators are generally non-linear functions of their parameters, hence the relation of the system on the input space is highly non linear [54, pp. 31–32].

A SA is normally preceded by an uncertainty analysis (UA), which quantifies the uncertainty on the output of the system by exploring the statistical properties of the system and its inputs [54, pp. 29–30]. The present study does not employ strictly an UA, because probability distributions of parameters and their uncertainties are not considered explicitly, a non-parametric space-filling approach is adopted instead. An estimation of uncertainties would be possible by employing multiple instances of the input space (e.g. bootstrapping, Monte Carlo methods). Additionally, uncertainties on climate data are considered only for projections, where a model ensemble is employed.

Results from this work highlight the importance of indicators parameters in a CCRA, e.g. thresholds [52, pp. 1873–1874]. The methods may be useful to authors of CCRAs to address the arbitrariness of parameters selection and to support the outcomes of the assessment. In this regard, the present study may found an application in climate services.

1.2 Climate data

Climate is a complex system, composed by many elements which interact in non-trivial (i.e. non-linear) ways. Therefore, to have a satisfying description of climate, many variables are needed. Climate data are data which can

be used to provide a direct or indirect description of climate,[7] e.g. in situ observations, measures from remote sensing or weather stations, outputs from numerical models [56, p. 1537]. The complexity of climate reflects on the complexity in structure of climate data, e.g. they can be represented as multidimensional objects and collected in climate datasets. This affects also their availability and other properties [28], therefore climate data can be regarded as big data.

To identify a subset of variables which efficiently describe the climate, the concept of essential climate variable (ECV) is defined [8]. The updated list of ECVs and their requirements are mantained by the World Meteorological Organization (WMO) in [4, pp. 14–17]. Climate data necessary for this study are among the present ECVs. In this section they are characterised mathematically, while the actual data are shown in section 3.

In the following, a generic ECV T can be represented mathematically as a scalar function

$$T : S_{\text{lat}} \times S_{\text{lon}} \times S_{\text{time}} \to \mathbb{R} \tag{1.1}$$

where S_{lat}, S_{lon} and S_{time} are domains of latitude, longitude and time dimensions, respectively.[8] Latitude and longitude are the only spatial dimensions considered, because elevation is specific to each ECV. In the following, when spatial dimensions are mentioned, they refer to the horiziontal dimensions of latitude and longitude. Every numerical value is equipped with proper unit of measurement, to represent physical quantities correctly. As a consequence, the codomain in equation (1.1) is partially wrong: with an abuse of notation, it represents only the magnitude of the ECV and does not consider the unit of measurement. This is a small exception to simplify the notation and in the remainder of this document units of measurement are always addressed explicitly.

A more practical representation of T is a multidimensional array, where values in the domain are coordinates associated to each dimension and each entry of the array is the result of T evaluated on those coordinates. Figure 1.2 shows this representation visually.

In the following, this representation is used to simplify the discussion and same ECV symbol is used both for the function and the multidimensional array.

[7] A note on nomenclature: the adjective *climatological* is used in some sources instead of *climate* to address to climate data. They are equivalent, but the latter is preferred in this work because it replicates the alternative term for normal specified by [3, p. 1].

[8] In contexts related to Machine Learning (ML) these objects are called tensors. Since they may not satisfy the mathematical definition of a tensor, in particular the map may not be multilinear and the numerical sets may not be vector spaces, no reference to such objects is made in this work.

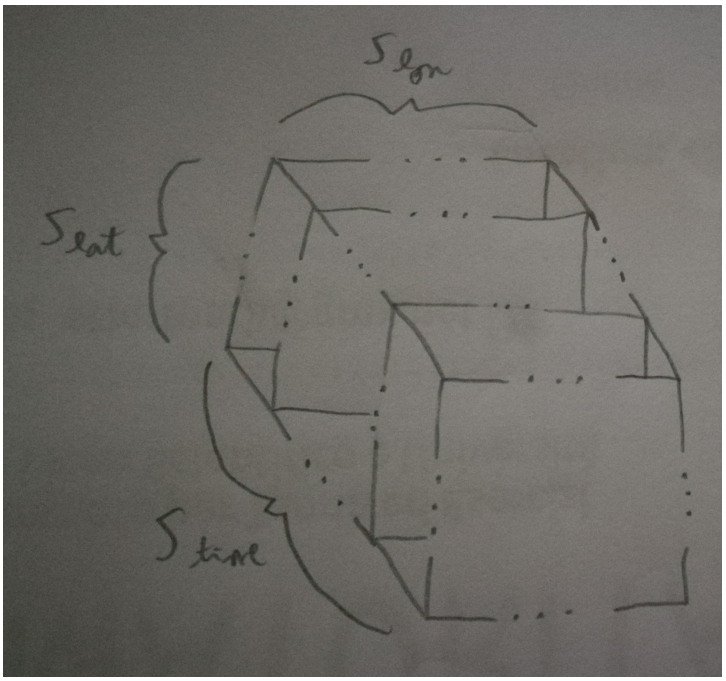

Figure 1.2: Representation of a generic ECV as multidimensional array.

Example

Near-Surface Air Temperature, symbol tas, is available for some coordinates $S_{\text{lat}} \times S_{\text{lon}}$ and timestamps S_{time}. It can be seen as the scalar function in equation (1.1), which associates each value in set $S_{\text{lat}} \times S_{\text{lon}} \times S_{\text{time}}$ to a scalar value with unit K, or it can be represented as the multidimensional array in figure 1.2, where each entry is function (1.1) evaluated at the corresponding coordinates.

As a visual aid when generic symbols are used, capital letters represent both functions and multidimensional arrays, the former being followed by the arguments in parentheses when there is an explicit reference to their values. Instead, lowercase letters are used for functions and values which are one dimensional.

A note on units of measurement: in atmospheric sciences and engineering applications it is common to use non-SI units because they are closer to everyday experience. Two notable cases in this work are: time expressed in number of days, $1\,\text{day} = 86\,400\,\text{s}$, and precipitation flux expressed as precipitation rate, with the implicit conversion $1\,\text{mm/day} = 1\,\text{kg/(m}^2\,\text{s)}\frac{86\,400\,\text{s/day}}{1000\,\text{kg/m}^3}$ using the density of water.

1.2.1 Climate normals

The temporal evolution of climate is described by climate data which can be represented as time series. To quantify changes in the state of climate it is useful to define a reference period and climate data related to it.

The concept of climate normal is introduced for this purpose, the WMO defines it as: *period averages computed for a uniform and relatively long period comprising at least three consecutive ten-year periods*, from [3, p. 2]. Terms period average and average apply to monthly values of climate data, see definitions and how normals are evaluated in [3, pp. 5–6]. However, the mean of values with other temporal domains may also be useful, e.g. multimonth normals, normal for each day of year of the wind speed at a given location. In the following the averaging period is expressed clearly. To quantify changes in the state of climate, anomalies are used, which are *the deviation of a variable from its value averaged over a reference period*, from [44, p. 2218].

In this work the reference period is a period of 30 years starting on 1st January of a year ending with the digit 1. This specification satisfies the definition of averaging period for climate normals. Instead, the boundaries are specific to the case study (see section 2.3.1).

In contrast to the reference period, averaging periods for future climate span 20 years and are fixed. Values referred to these periods describe the system or the climate at future time horizons, which is an useful information for any planning involving the system [14, p. 23]. The lower number of years in these periods do not affect negatively the prediction skill of statistics related to them [3, p. 17].

1.3 Indicators

Indicators of drivers within the hazard determinant are functions of climate data and additional parameters. In this work the climate data are ECVs and they have a daily frequency. During their calculation, generally indicators are aggregated over the temporal dimension and are non-linear functions of their arguments. An indicator I can be defined mathematically as

$$I : S_{\text{lat}} \times S_{\text{lon}} \times S_{\text{y}} \times \prod_{p \in P_I} S_p \to \mathbb{R} \tag{1.2}$$

where S_{y} is a set of the years considered during the analysis, P_I is the set of parameters for that indicator and S_p is the set of values available for each parameter $p \in P_I$.[9] In the following, $\underline{z} \in \prod_{p \in P_I} S_p$ represents the set of arguments passed to the indicator, in other words the coordinates of I as multidimensional array. Evaluation is performed for each year, i.e. the

[9] As a symbolic shortcut, if $P_I = \varnothing$ then the indicator is defined only over $S_{\text{lat}} \times S_{\text{lon}} \times S_{\text{y}}$.

indicator has yearly resolution or is evaluated with yearly frequency. As a consequence, the elements of set S_{y} are references to the years taken into account during calculation.

An indicator can be represented as a multidimensional array, similarly to ECVs. The dependence of an indicator on ECVs is not clear in the definition given by equation (1.2), but in the following this is made explicit by the context or by the definition of the indicator.

Example

The indicator $\mathrm{TX_x}$ is evaluated for the period 1991-2020 with yearly frequency. This indicator is the monthly maximum value of daily maximum temperature [25], hence:

- it depends on ECV Maximum Near-Surface Air Temperature defined at daily frequency over the considered period,

$$S_{\mathrm{time}} = \left\{ t : \begin{array}{l} t \text{ day from 1st January 1991} \\ \text{to 31st December 2020} \end{array} \right\} \quad ;$$

- spatial dimensions are not specified, hence the evaluation is performed for each point of an arbitrary set $S_{\mathrm{lat}} \times S_{\mathrm{lon}}$;
- no additional parameters are required, $P_{\mathrm{TX_x}} = \varnothing$;
- the outcome is a scalar value for each year in the period,

$$S_{\mathrm{y}} = \{1991, 1992, \ldots, 2020\} \quad ;$$

- the multidimensional array representation of the indicator is in the following figure, where each entry is a real value with unit K:

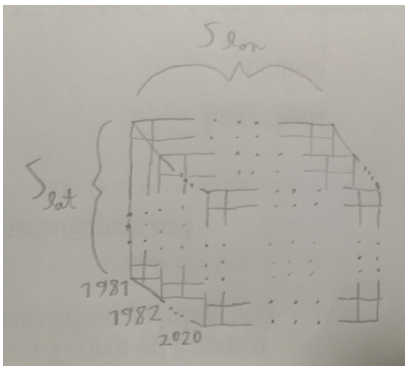

Indicators of drivers within exposure and vulnerability determinants may be defined similarly as the hazard determinant as scalar functions depending

on specific variables characterising the system.

1.4 Structure of the document

Each section of the document treats a different aspect of the analysis. A general understanding of the concept of risk and the associated terms are necessary to frame the problem. They are exposed in chapter 1, along with useful concepts on climate and a mathematical description of climate data and indicators.

Data specific to the study and any elaboration applied to them are then presented in chapter 2. Section 2.3 in particular describes the methodology of CCRA which is followed in this work.

Results of the application of the methodology to the case study and the consequent SA are in chapter 3, while chapter 4 summarises the final considerations on this study and points of departure for future studies.

Example boxes are present after some paragraphs of the document to provide a practical example of the use of the explained concepts. Examples are unrelated to the thesis, in the sense that the important content is explained in the main text.

Chapter 2

Data and Methods

2.1 Reference dataset

The climate dataset used for evaluating reference values is ERA5 by European Centre for Medium-Range Weather Forecasts (ECMWF) [35]. ERA5 is a reanalysis dataset, which provides gridded data with global coverage and hourly temporal resolution. Reanalyses are observations of climate data interpolated on a spatiotemporal grid throught numerical models, a procedure called data assimilation (see [36] for technical details). The main technical data about ERA5 can be found in table 2.1.

In this work the ERA5 horizontal resolution of 0.25°, i.e. about 31 km, is used for both latitude and longitude. In the dataset, horizontal coordinates of a grid point natively refer to the upper left angle of the cell. A traslation is applied to refer these coordinated to the centre of the cell.

On the temporal dimension, climate data from 1st January 1950 to 31st December 2023 are selected from ERA5. First, data are converted to a calendar with 365 days by removing 29th February in leap years. Then they are downsampled to daily resolution with the same aggregation procedures specified by WMO for the evaluation of individual monthly values from daily values [3, p. 5]. In particular:

- daily Near-Surface Air Temperature is the mean of hourly Near-Surface Air Temperature of the same day;

Table 2.1: Subset of the technical characteristics of ERA5, the complete list can be found in [36, p. 2003].

Characteristic	Value
Horizontal coverage	global
Horizontal resolution	0.25° longitude-latitude
Temporal coverage	from 1st January 1940 to present
Temporal resolution	hourly

- daily Maximum Near-Surface Air Temperature is the maximum of hourly Maximum Near-Surface Air Temperature of the same day;
- daily Minimum Near-Surface Air Temperature is the minimum of hourly Minimum Near-Surface Air Temperature of the same day;
- daily Precipitation is the sum of hourly Precipitation of the same day.

Timestamps for daily data are set at midnight.

2.2 Climate projection dataset

Future climate is studied using the NEX-GDDP-CMIP6 dataset provided by NASA Earth Exchange (NEX) [61, 62]. The dataset is derived from results of Coupled Model Intercomparison Project Phase 6 (CMIP6) for a subset of ECVs and a single variant of 35 models from a selection of historical and ScenarioMIP experiments [27].

Models are numerical representations of the climate and in general are called general circulation models (GCMs) or Earth system models (ESMs) when advanced processes of Earth are included (e.g. biological processes and feedbacks in EC-Earth3, see [22]). Models working at smaller scales are available: they can be used to dynamically downscale the projections, but they propagate existing systematic errors from the GCMs and introduce new ones, e.g. biases related to the topography in extremes of temperature [56, pp. 1551–1552]. Methods to correct these errors are available but with the disadvantage to lose information on global processes given by GCMs and the physical interpretation of outputs [23]. Therefore only models at the global scale are used in this work.

The purpose of having a set of different models from NEX-GDDP-CMIP6 is to evaluate the uncertainty on predictions, in fact each model has different characteristics and applying ensemble methods reduces the variance on the outputs given by model-specific characteristics (e.g. different equations describing the same phenomena, different modules between models). NEX-GDDP-CMIP6 provides a single variant for each model. Data are obtained through statistical downscaling and bias adjustment procedures presented in [60]. The main technical data about NEX-GDDP-CMIP6 can be found in table 2.2, while the full description of the dataset is in [61].

The spatial resolution of this dataset matches the resolution of ERA5 and horizontal coordinates identify the centre of grid points, hence no further rescaling is required.

Data of NEX-GDDP-CMIP6 have daily resolution but timestamps are referred to noon of the coordinate. This does not raise problems when operations are applied to data aggregate at lower frequencies, e.g. monthly averages, but may create contradictions in pointwise calculation. Therefore,

Table 2.2: Subset of the technical characteristics of NEX-GDDP-CMIP6, see [61] for the full specifications.

Characteristic	Value
Horizontal coverage	global
Horizontal resolution	0.25° longitude-latitude
Temporal coverage	from 1st January 1950 to 31st December 2100
Temporal resolution	daily

timestamps in NEX-GDDP-CMIP6 are redefined to match the timestamps or ERA5, i.e. midnight. The temporal coverage is split between historical and future experiments. The historical simulation starts at 1st January 1950 and ends at 31st December 2014, while the projections are from 1st January 2015 to 31st December 2100.

In this work some models are excluded, reasons for exclusion are in appendix A.1 along with the list of used models. For each model, the following experiments are considered:

historical simulation of the past climate;

SSP1-2.6 low emission scenario, with low challenges in mitigation and adaptation to climate change;

SSP2-4.5 intermediate scenario, with moderate challenges;

SSP3-7.0 high emission scenario, with high challenges.

More details on the narratives of each Shared Socioeconomic Pathway (SSP) are found in [47]. The use of SSP scenarios allows to account for the evolution of socioeconomic elements which may affect indirectly the system. In each model the historical experiment is extended up to 31st December 2023 using data from the SSP2-4.5 experiment. This procedure is suggested by [27, p. 1954] and allows to compare historical data from models with the reference dataset, in what can be considered the *past* of the study, while the *future* starts at 1st January 2024.

Non-physical temperature extremes

At the time of writing, NEX-GDDP-CMIP6 dataset contains some values of Minimum Near-Surface Air Temperature and Maximum Near-Surface Air Temperature which are not accettable from a physical perspective, i.e. tasmin > tasmax, for the same days and some models.[1]

[1] Also Near-Surface Air Temperature occurs to have non-physical values, i.e. tas < tasmin or tas > tasmax. However, this issue is not addressed explicitly, since every chosen indicator having temperature variables as inputs does not require tasmin or tasmax to be used together with tas.

The issue appears as a rare by-product of the bias adjustment algorithm employed in the dataset creation, see [60]. It does not affect calculation on normals since they are monthly means, but for resolutions on the order of days may be conditioned negatively by the non-physical value. To be able to recover those data helps to maintain accurate information on the distribution of extremes and its evolution due to climate change, see [56, pp. 1536–1537] and [29, pp. 40–42].

From a discussion with the providers of the dataset, the suggested course of action is to swap tasmin and tasmax values for data presenting the problem.

2.2.1 Bias adjustment

Outputs of GCMs and the more advanced ESMs have intrinsic biases related to their functioning (e.g. implementation, physical equations, parametrisations) which need to be adjusted to convey physically accurate values, essential for studies like CCRAs.[2] A moltitude of BA methods are available, e.g. deviations from reference data, statistical analysis, ML models [12, 49, 46].

When BA is performed on climate data, a reference is chosen. The reference data are assumed to be a representative sample of the population, hence the sample distribution of reference data describes the probability distribution of the climate data accurately. The BA procedure extracts information on statistics of reference data and modifies the climate data to reproduce those statistics. In fact, biases are considered alterations of the true probability distribution induced by the models and BA aims to remove them. Moreover, climate change affects the probability distributions making them non stationary. This means that statistical information in a given temporal period may not be accurate to describe data in future periods, even if they are extracted from the reference data. Some BA procedures address this issue.

In this study the BA algorithm known as Quantile Delta Mapping (QDM) is adopted [12]. It belongs to the family of Quantile Mapping (QM) algorithms for BA, which use statistical information from quantiles of reference data to remove the bias. QDM is able to preserve trends of climate change detected by the GCMs, by storing the difference by quantile of future periods with respect to an historical period. Depending on the climate data, the relative change may be stored instead of the absolute difference.

As explained in [12, pp. 6941–6942], QDM estimates three empirical quantile functions (QFs): one for the climate data to adjust, one for the reference data and one for the climate data in the same period of reference data. Then differences between same quantiles of climate data at different

[2] In many resources on the topic, the term *bias correction* is used instead. Here bias adjustment (BA) is preferred since a correction requires a true value as reference, which is not always possible to assume.

temporal periods are stored. The actual adjustment consists in replacing target climate data with the corresponding quantiles from the reference data and adding back the differences stored previously.

The mapping between the empirical QFs in the common period may be interpreted as the training step of the BA algorithm. Moreover, the procedure requires to invert the QFs, i.e. to evaluate the corresponding empirical cumulative distribution functions (CDFs) of data, to map quantiles to their probabilities.[3]

Concerning this study, the reference distribution is built on ERA5. The period from 1st January 1950 to 31st December 1993 is chosen to extract the information needed for BA. Then the 30-years period from 1st January 1994 to 31st December 2023 is used to test the accuracy of the BA procedure. The BA is applied to ECVs of each model in NEX-GDDP-CMIP6. A q-q plot is made to compare the adjusted data against the reference data.

Temperature

QDM is applied additively to temperature data. This means that to conserve trends between projections and historical data, the absolute difference between quantiles is stored.

Temperature data subject to adjustment are ECVs tas, tasmin and tasmax. In particular, first tasmax and the Diurnal Temperature Range

$$\mathrm{DTR} = \mathrm{tasmax} - \mathrm{tasmin} \tag{2.1}$$

are adjusted, then the adjusted tasmin is derived by inverting equation (2.1). Since the reason of the non-physical extremes problem is not addressed yet (cf. section 2.2), the absolute value of the adjusted DTR is considered. This is equivalent to swap the adjusted tasmin and tasmax when tasmin $>$ tasmax. This procedure is suggested in [60, p. 3313] with the addition of the swap of non-physical extremes.

Precipitation

For precipitation data, trends are preserved by storing the ratio of projected data with respect to historical data, i.e. multiplicative QDM is applied. The adjustment is applied to Precipitation pr. However, null values are present in the datasets, which correspond to days without any kind of precipitation, i.e. dry days. When they appear in the historical data, the trend-preserving ratio diverges to infinity, resulting in a non-physical infinite value of the adjusted pr.

The procedure suggested in [12, p. 6945] is followed to solve the issue: values lower than the threshold 0.05 mm/day are randomised uniformly in the

[3] More properly they are sample frequencies instead of probabilities, but for clarity the latter term is used.

interval (0 mm/day, 0.05 mm/day), then after the BA the values which are below the threshold are considered dry days, hence they are set to 0 mm/day. No correction in the seasonal cycle is applied since only daily data are needed for the evaluation of indicators.

2.3 Methodology of risk assessment

Restricting the risk assessment to climate-related applications is not sufficient to fix every detail, e.g. how to evaluate risk from its determinants. These implementation details are often expressed in the methodology chosen to perform the risk assessment. The methodology employed in this study is presented conceptually in these paragraphs and defined operatively in sections 2.3.2 and 2.3.3.

The methodology is split into eight modules, each dependent on the previous ones. The following is an overview:

1. understand the context in which the assessment is framed and identify objectives, scope and resources involved [59, pp. 39–53];
2. identify risks and impacts affecting the system under study and determine drivers of hazard, exposure and vulnerability [30, pp. 26–41];
3. choose indicators for each driver of hazard, exposure and vulnerability [59, pp. 73–84];
4. collect data and quantify indicators [59, pp. 87–103];
5. normalise indicators to allow their comparison [59, pp. 105–119];
6. for each determinant, weight normalised indicators and aggregate them into a single value [59, pp. 121–131];
7. aggregate values for individual determinants into a single value for risk [59, pp. 133–141];
8. present the results of the CCRA [59, pp. 143–154].

When the vulnerability of the system is recalled, it is split into sensitivity and adaptive capacity if possible.

All modules are connected by the concept of impact chain, which is an *analytical approach that enables understanding of how given hazards (3.8) generate direct and indirect impacts (3.14) which propagate through a system (3.3) at risk (3.13)*, from [41]. This concept helps to develop the CCRA as a narrative and to guide it smoothly through its various steps, see [42, pp. 217–224] for a review of the concept.

Although a complete application of this methodology does not fall into the purposes of this study, each module is briefly addressed in the following

Table 2.3: Drivers of hazard with their symbols.

Driver	Symbol
Heat wave	HW
Heavy precipitation	HP

sections and results of evaluations are presented in section 3 where case studies are treated.

2.3.1 Impact chain

This section presents briefly scope and objectives of the CCRA as indicated by module 1 of the methodology. There is no direct involvement of experts and stakeholders, but literature provides for information on context and objectives for the case study. Moreover drivers are introduced, as requested by module 2.

The present work is applied to impacts of climate change on airports. The aviation sector is a complete test case for responses to climate change: it implements reduction of negative impacts on infrastructures and transport network through adaptation measures as well as mitigation of the adverse effects on climate originated from sectorial activities [39]. The disruption of critical infrastructures such as airports have important consequences on mobility and economic growth (see [38], [11, p. 15] and [19, p. 548] for a review of impacts). Hence, the estimation of climate risk for airports becomes an essential tool for effective planning and risk management.

Impacts from extreme temperatures and precipitation are studied, as they are among the biggest challenges to address in the aviation sector. Both International Civil Aviation Organization (ICAO) and WMO collected opinions and experiences from stakeholders through surveys [38, p. 62] and [2, p. 34], respectively. More in detail, the two hazard drivers heat wave and heavy precipitation are considered. They are selected from the taxonomy provided by European Union for CCRA, to have a well-known and authoritative reference in the field [16, p. 177], and both drivers are associated to acute physical risks. A symbol is associated to each driver to track their use in the calculations, see table 2.3.

An heat wave is defined by IPCC as *a period of abnormally hot weather, often defined with reference to a relative temperature threshold, lasting from two days to months. [...]*, from [44, p. 2233]. WMO presents a similar definition, highlighting the lack of a universally accepted definition, which is replaced by local criteria, although it would facilitate the exchange of information between stakeholders [1, p. 5]. Heat waves have a wide range of impacts, particularly at the regional scale for airports, e.g. higher temperatures may damage runways or decrease the efficiency of cooling systems, changes in air density affect the runway length required for airside opera-

Table 2.4: Drivers of exposure considered in the study and associated indicators. The part of the table above the line shows the air-side components, below the line there are the land-side components. Dimensionless quantities have an empy cell in the Unit column.

Driver	Symbol	Indicator	Unit
Runways	e1	area	m^2
Terminals	e2	area	m^2
Offices and other buildings	e3	area	m^2
Carparks	e4	number	

tions, increased humidity translates in more fog in earlier hours of the day [38, pp. 23–28].

For IPCC *an extreme/heavy precipitation event is an event that is of very high magnitude with a very rare occurrence at a particular place. [...]*, from [44, p. 2229], where the term *precipitation* refers to water in every state, e.g. rain, snow, ice. Further details on the characterisation of heavy precipitation are provided by WMO in [1, pp. 6–7]. Climate change shifts local and global distributions of rainfall [56, p. 1605]. These impacts are likely to occur in the near future and the one affecting airports are local in nature, e.g. flooding due to failures in drainage systems, but they may propagate throughout the aviation network depending on their severity [38, pp. 28–34].

Exposure drivers in airports are the physical components of the airport. They can be subject to impacts of climate change at various levels, hence their presence determines risks. Normally the components of airports are divided in air side and land side, the former regarding all components which interact with aircraft operations and the latter for the public areas [19, p. 553]. This distinction is made for helping the collection of data on drivers. In this study the considered drivers are listed in table 2.4 and they are taken from [19, p. 554]. A single indicator is chosen for every driver, they are listed in the same table and are identified with the same symbol to simplify the notation.

Vulnerability data are divided in adaptive capacity and sensitivity. Under adaptive capacity are gathered measures which are active, planned or not present for the system in order to contain negative impacts of climate. Instead, drivers of sensitivity are elements of the system subject directly to the realisation of risks. Drivers are derived from [19, pp. 555–556, 558] and are listed in table 2.5. Similarly to the exposure determinant, the table shows also vulnerability indicators because a single indicator is chosen for every driver, hence they can be identified by the same symbol, for ease.

The CCRA analyses a square box 3 grid cells wide centered approxi-

Table 2.5: Drivers of vulnerability and their indicators. Specifically, drivers of adaptive capacity are above the line, while drivers of sensitivity are below. Dimensionless quantities have an empty cell in the Unit column.

Driver	Symbol	Indicator	Unit
Risk awareness	v1	level	
Guidelines for adaptation plan to climate change	v2	presence	
Efficient drainage system	v3	presence	
Monitoring and alarm system	v4	presence	
Bioinfiltration and permeable pavements	v5	presence	
Soil sealing	v6	area	m^2
Passengers	v7	number	
Age buildings	v8	number	
Air traffic	v9	number	
Underground infrastructures	v10	area	m^2

mately at the coordinates of the system. The systems studied in this work have spatial scale much smaller than the size of a grid cell, hence it is guaranteed that the central grid cell encompasses the systems, even if the coordinates of the centre of the system are not accurate. Although one grid cell is enough to cover the systems under study, an extended area is chosen to increase the predictive skill of aggregation procedures applied to the spatial dimensions. On the other hand, the CCRA would lose spatial accuracy in the description of the local events around the system, if too many grid cells are selected. Since reference and projections datasets have same spatial resolution and coordinates (cf. sections 2.1 and 2.2), same coordinates are considered for the system under study.

The reference period covered by the CCRA of this study is chosen such that it precedes the start of the formation of the system or anticipates major changes to its structure. This arbitrary criterion is chosen to compensate the natural deteriotation of materials, with artifical buildings in mind. In fact, the methodology implicitly assumes that exposure and vulnerability values are either constant in time or their change is negligible within the period they refer to. This hypothesis and the definition of the reference period together guarantee that there is no correlation in time between quantities referring to different temporal periods considered in the CCRA.

Example

Suppose the system under study is the Eiffel Tower. The works started in 1887 and lasted two years, hence

$$S_{\text{time}}|_{\text{ref}} = \{t : t \text{ day from 1st January 1851 to 31st December 1880}\}$$

is chosen as reference period. Normals can be evaluated for the climate data referred to $S_{\text{time}}|_{\text{ref}}$ and data related to the system describe it as if it would not be affected by the passing of time.
If the period from 1st January 1861 to 31st December 1890 were chosen instead, no assessments could be produced for the years subsequent to the end of works.

The future climate is described for three time horizons, they are summarised in table 2.6. Near and medium-term time horizons are chosen to be as close as possible to the present (at time of writing). This way it is more reasonable to find adaptation plans and strategies for the system at risk. Long-term time horizons are affected by greater uncertainty for different reasons, e.g. lower confidence on outputs from climate projections, exposure subject to change. Nevertheless, the long period is chosen to show differences between scenarios, which are more evident at the end of the century for many ECVs.

Table 2.6: Time periods used in the analysis to describe future climate and the evolution of risk.

Time horizon	Symbol	Start	End
Near	near	1st January 2024	31st December 2043
Medium	medium	1st January 2044	31st December 2063
Long	long	1st January 2081	31st December 2100

2.3.2 Evaluation of indicators

This section explains the process to obtain a scalar value for each determinant, following the methodology presented in section 2.3. Modules 3, 4, 5 and 6 are recalled. The following paragraphs are further split in logical groups to help to follow the whole process. Although the selection of drivers for the actual case studies is presented in section 2.3.1, formulae involving drivers and indicators are kept general.

Choose the indicators

Module 3 may be stated symbolically as follow. For each driver within the hazard determinant, a set $\mathcal{H}_j$ of indicators is obtained. A similar procedure is carried out for drivers of exposure and vulnerability, resulting in sets $\mathcal{E}_i$ and $\mathcal{V}_k$, respectively. Indices i, j and k are present to clarify that each set is related to a different driver and the way these sets are indexed is not important (e.g. each of them can be a sequence of integers where each one refers to a different driver, they can be the names of the drivers they refer to). If the distinction between drivers of sensitivity and adaptive capacity is made, then it is not explicit in the indices. The reason is that these drivers are treated mathematically the same way, as explained below.

Note that in module 3 no evaluation is performed yet, hence the elements of each set are just scalar functions. In other words, they are just descriptions of how they quantify the driver.

The methodology suggests to avoid double counting of drivers by allocating each of them in one determinant only [30, p. 29]. This implies to have different indicators, even if they are defined in a similar way.

Example

The risk of water scarcity affecting a location is assessed. This example is inspired by [30, p. 46]. The system is the location under study.
One driver of exposure and two of vulnerability are chosen, they are respectively:

exp1 presence of farmers in the region;

vul1 insufficient know-how about irrigation systems;

vul2 weak institutional setting for water management.

Both drivers of vulnerability describe the adaptive capacity of the system. All drivers are conveniently identified by lables.
An indicator for each driver is chosen, the resulting sets are:

$$\mathcal{E}_{\text{exp1}} = \begin{Bmatrix} \text{“number of farmers in the region”} \end{Bmatrix} ,$$
$$\mathcal{V}_{\text{vul1}} = \begin{Bmatrix} \text{“number of farmers trained in improved irrigation techniques”} \end{Bmatrix} ,$$
$$\mathcal{V}_{\text{vul2}} = \begin{Bmatrix} \text{“number of local water co-operations”} \end{Bmatrix} .$$

Note that all indicators consist in counting some elements of the system. Nevertheless, they are different from each other since they refer to different elements, hence the drivers are different.

In particular for this study, an heat wave is described mathematically by indicators in table 2.7. Heat waves are described both in frequency and duration, through HWI and HWML, respectively. Indicators in table 2.8 are chosen to describe an heavy precipitation event. Other than duration and frequency, estimated by CWD and Rp5mm, respectively, also the intensity of the event is quantified by Rxp4day. All indicators are generalised versions of indicators and indices frequently used in literature, e.g. [32, p. 2208]. They are provided by [9] and are evaluated at yearly resolution.

In module 4 the evaluation of indicators on climate and system data occurs. Concerning the system, the data collection step is explained in section 2.3.1 and scalar values are readily obtained for the elements in sets $\mathcal{E}_i$ and $\mathcal{V}_k$ for any driver i or k. See paragraphs about data in section 2.3.1 for the definition of the indicators of exposure and vulnerability used to describe each system and section 3 for their values.

A more convoluted path is needed to evaluate indicators of hazard. They are functions defined by equation (1.2), hence they depend on climate data and additional parameters. In tables 2.7 and 2.8 parameters are listed to

Table 2.7: Indicators describing heat wave events. They have yearly resolution.

Indicator	Symbol	Unit	Arguments	Definition
Heat wave index	HWI	day	tasmax, p1, p2	Total number of days in sequences of at least p1 consecutive days with tasmax > p2
Heat wave max length	HWML	day	tasmin, tasmax, p1, p2, p3	Maximum number of days in sequences of at least p1 consecutive days with tasmax > p2 and tasmin > p3

Table 2.8: Indicators describing heavy precipitation events. They have yearly resolution.

Indicator	Symbol	Unit	Arguments	Definition
Maximum consecutive p4-day precipitation	Rxp4day	mm	pr, p4	Maximum cumulative precipitation in sequences of at least p4 consecutive days
Wet days	Rp5mm	day	pr, p5	Total number of days with pr $\geq$ p5
Maximum length of wet spell	CWD	day	pr, p5	Maximum number of consecutive days with pr $\geq$ p5

complete the definition of indicators, but they are detailed in the following paragraphs.

Choose the values of parameters

For each indicator, a set of values of its parameters is defined. Ideally these sets would be continuous, to explore the whole space of possible configurations of parameters. However, for limitations intrinsic to the analysis tools, only a finite and small number of values can be considered. In the following these discrete sets are called intervals to preserve generality. How values in these intervals are selected depends on the nature of the parameters. The selection is ultimately arbitrary, to allow greater control, e.g. remove values which are not interesting for the analysis, and to apply a form of non-parametric sampling of the input space. This is a form of space-filling design for SA [20, pp. 593–594].

To simplify the explanation, consider driver j and an indicator $I \in \mathcal{H}_j$. This indicator depends on some parameters, which are collected in set P_I, and on some ECVs. The chosen interval for a parameter $p \in P_I$ is a set of scalar values, possibly with units of measurement, denoted by S_p.

If parameter p is related to a ECV (e.g. Threshold of tas), its values are sampled from the distribution of the ECV. First all data available for the ECV of interest are collected in a single sample, with the following conditions:

- temporal coordinates belong to the averaging period $S_{\text{time}|\text{ref}}$ chosen for the normals;
- spatial coordinates are ignored.

This procedure has the side effects of removing the dependence of parameter values from spatial and temporal coordinates and to increase the sample size. The sampling is not affected by existing spatial correlation between data, because it is non parametric and regards only the possible values of the ECV and not their spatial distribution. In fact, the probability of having any value v for the ECV T in the sample is

$$\mathcal{P}(v) = \frac{1}{|S_{\text{lat}}||S_{\text{lon}}||S_{\text{time}|\text{ref}}|} \sum_{y \in S_{\text{lat}}} \sum_{x \in S_{\text{lon}}} \sum_{t \in S_{\text{time}|\text{ref}}} \mathbb{I}[T(y,x,t) = v] \quad . \quad (2.2)$$

It is a frequentist probability and gets more accurate the larger the sample size is, by definition. Second, the empirical QF of data is built from the sample, to acknowledge the shape of their true probability distribution. Minimum and maximum values are treated as the first and last quantiles, respectively. Since the number of data is large but limited, this curve is an approximation of the inverse function of the CDF and missing data are interpolated linearly. Third, values are chosen with the aim to sample the true probability distribution uniformly, starting from the quantile corresponding

to frequency 90%. This allows to focus the analysis on the side of the distribution which have higher values, related to extreme risks. The density of points may be increased where needed to have a better description of the shape of the distribution.[4]

If parameter p is not related to a ECV, e.g. window size for moving averages, some heuristic is applied and explained case by case where values are presented in section 3.

The parameters indicators chosen for this study depend on are collected in table 2.9. Note that despite the definition of heat wave lasting two or more days, a window of one day is considered, i.e. p1 = 1, simply to count the number of days with extreme temperatures in a year. In particular, indicator HWI becomes TXnn, see [32, p. 2209]. Actual values displayed with uncertainty from the ensemble average are collected in section A.2.

Evaluate the indicators

After S_p is defined for every $p \in P_I$, the indicator I is finally evaluated. This results in elements of set $\mathcal{H}_j$ being multidimensional arrays given by equation (1.2), for every driver j of the hazard. Different indicators may have different parameters, but they depend on ECVs which same spatial and temporal coordinates $S_{\text{lat}} \times S_{\text{lon}} \times S_{\text{time}}$, hence they have same temporal frequency, i.e. same S_{y}.

From a computational perspective, the time complexity for the evaluation of an hazard indicator I is a particular function f of the number $|S_{\text{time}}|$ of temporal coordinates of climate data.[5] The evaluation is then repeated for every spatial coordinate in $S_{\text{lat}} \times S_{\text{lon}}$, year in S_{y} and combination of parameters $\underline{z} \in \prod_{p \in P_I} S_p$. In symbols the time complexity is

$$O\left(f\big(|S_{\text{time}}|\big)|S_{\text{lat}}||S_{\text{lon}}||S_{\text{y}}| \prod_{p \in P_I} |S_p| \right) \quad . \tag{2.3}$$

For indicators in table 2.9, the evaluation time of an indicator for a single choice of its arguments can be always bounded by polynomial functions, $f\big(|S_{\text{time}}|\big) = \big(|S_{\text{time}}|\big)^a$, with $a \in \mathbb{R}$ specific to the indicator being evaluated. This means that the computation benefit from a parallel setup.

Indicators are also evaluated for each model available (see table A.1). A different model may have different values for an ECV at the same coordinates. Moreover, these differences reflect on the procedures of evaluation of

[4] Why do not use derivative-based methods to set the density of points? The reason is again greater control on the selected values: there is no need to evaluate the derivative of the QF in every point, just within the subintervals which are interesting for the analysis. Note that the QF is obtained by linear interpolation between existent data values, hence the slope is already evaluated internally and the derivative is a piecewise constant function.

[5] Here time complexity is intended as number of steps of an algorithm, which can be related to physical time when executed on a calculator.

Table 2.9: Parameters present in the definitions of hazard indicators.

Parameter	Symbol	Unit	Interval
Consecutive days of extreme temperature	p1	day	Integer numbers from 1 to 31 in steps of 3
Threshold of tasmax	p2	°C	Quantiles of order 0.90, 0.97, 0.99, 0.999, 1.0 of tasmax in the reference period
Threshold of tasmin	p3	°C	Quantiles of order 0.90, 0.97, 0.99, 0.999, 1.0 of tasmin in the reference period
Consecutive days of extreme precipitation	p4	day	Integer numbers from 1 to 31
Threshold of pr	p5	mm/day	Quantiles of order 0.90, 0.97, 0.99, 0.999, 0.9999 of pr in the reference period

parameters values. Therefore, it is better to address to quantiles of ECVs as their sample frequency rather than their value.

Some combinations of parameter values are excluded from the calculations because they may bring to inconsistent results. Moreover, this issue could be present only for some models, due to their variability. The operation of removing these invalid combinations has the two advantages of reducing the number of calculations and removing values of indicators which may seem plausible but have no physical meaning because derived by unallowed physical conditions.

In this work the combinations having p3 > p2, i.e. the Threshold of tasmin greater than the Threshold of tasmax are removed. Although this condition is not problematic per se, it could allow events of heat wave with tasmin > tasmax and it is not physically acceptable. Among the model considered for this study, six present combinations of this kind. In particular, all these models have the maximum of tasmin, i.e. quantile of order 1.0, greater than quantile of order 0.9 of tasmax. Between the two quantiles, the former is removed, to have more variability over coordinates S_{p2}: the expectation is to study a wider range of effects on risk, since two indicators depend on Threshold of tasmax p2 instead of one for p3. See table A.2 for the list of models involved. All the combinations containing the specific value of parameter p3 are deleted, to streamline the following computational procedures.

The results of the initial computation of indicators need further elaboration. In fact, for every driver i and k, $\mathcal{E}_i$ and $\mathcal{V}_k$ contain scalar values which encapsulate information about the system for the chosen time period and system without reference to spatial coordinates. To obtain an analogous result for drivers of hazard, indicators are aggregated over spatial and temporal dimensions. For simplicity intermediate results are identified with the same variable I.

Aggregate the temporal dimension

First, the temporal aggregation is performed. It consists in averaging the multidimensional array over the temporal dimension with a sample average. The outcome is multidimensional arrays depending on spatial coordinates and parameters:

$$I(y, x, t, \underline{z}) \mapsto I(y, x, \underline{z}) = \frac{1}{|S_{\mathrm{y}}|} \sum_{t \in S_{\mathrm{y}}} I(y, x, t, \underline{z}) \quad . \tag{2.4}$$

Figure 2.1 shows one of the results of the aggregation for indicator HWML. Climate data for coordinates related to the case study are used and the aggregation is performed over the reference period. To display the spatial distribution, indicator parameters are fixed to specific values. This representation of data is useful to focus on spatial characteristics of climate data

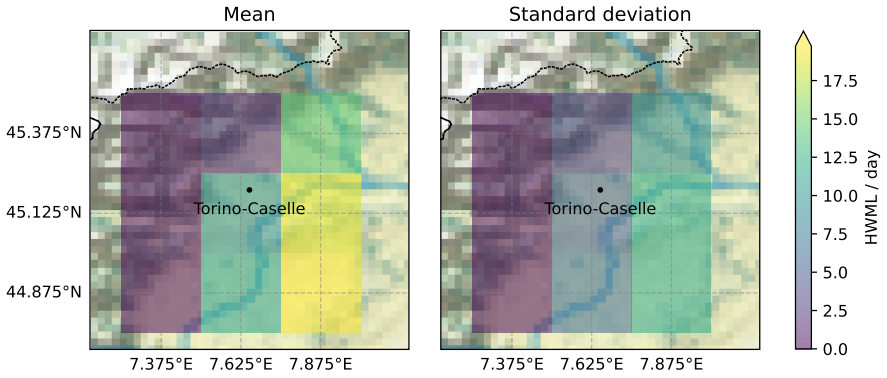

Figure 2.1: Heat wave max length (symbol HWML, unit day) indicator temporally aggregated on the reference period for the EC-Earth3 model. Sample average and sample standard deviations are shown as spatial distributions with fixed parameters p1 = 4 day, p2 = 24.67 °C and p3 = 15.32 °C, both thresholds of temperature are the 90th percentile. The black dot is the reference point of the case study. Effects of orography are visible, reducing daily tas in grid cells covering mountain ranges.

which could affect indicators. The sample standard deviation over time, i.e. evaluated with respect to the sample mean and normalised with $|S_y| - 1$, is displayed to give more information on the temporal distribution of data at each grid cell. It is not used further because it may not consider uncertainties specific to the models, which are taken into account with an ensemble average at the final steps of the analysis instead.

EC-Earth3 is one of the models being affected by the issue of Threshold of tasmin being larger than the Threshold of tasmax for some values. To apply the temporal aggregation in these cases, the missing coordinates are ignored and the sample average is performed on a reduced sample.

Due to the spatial resolution of data, they may contain bias with respect to the reference period, e.g. orography may influence differently the variation of some ECVs as can be seen in figure 2.1. A useful quantity to study this phenomenon is the variation of any indicator I with respect to the reference period,

$$I(y, x, \underline{z}) - I|_{\text{ref}}(y, x, \underline{z}) \quad , \tag{2.5}$$

where symbol $I|_{\text{ref}}$ is used to refer to I evaluated for the reference period, i.e. equation (2.4) with average over set $S_y|_{\text{ref}}$.[6] This is analogous to evaluate anomalies for indicators instead of ECVs. Since data for all time points are available for each year, a sample average is performed on al data, instead of

[6] Another similar quantity is the relative difference with respect to the reference period, i.e. the anomaly divided by $I|_{\text{ref}}(y, x, \underline{z})$. This is not chosen because some indicator values are exactly 0, e.g. for integer-valued indicators, resulting in mathematically undefined quantities which have no meaning.

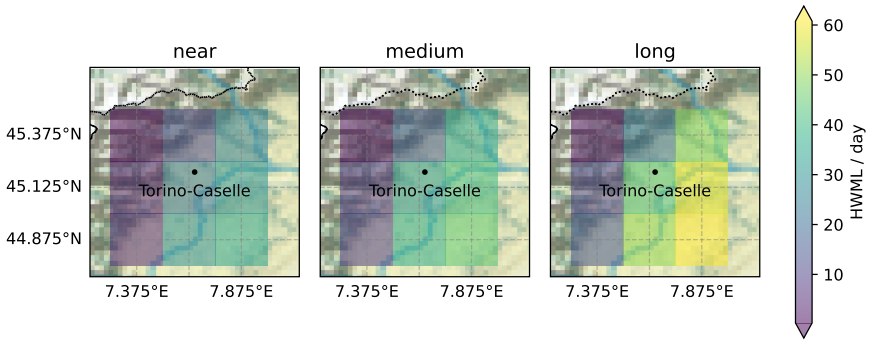

Figure 2.2: Anomalies of Heat wave max length (symbol HWML, unit day) indicator for each time horizon with respect to period 1971-2000, i.e. the reference period selected for the use case. The spatial distributions are result of the temporal aggregation of indicators. Data refer to the case study and are from the SSP2-4.5 scenario experiment of the EC-Earth3 model. Parameters have values p1 = 4 day, p2 = 24.67 °C and p3 = 15.32 °C, both thresholds of temperature correspond to the 90th percentile. In general the number of heat wave events increases and spatial differences caused by orography are accentuated with time.

splitting the evaluation first on months as suggested by [3, p. 6]. An example of indicator anomaly is shown in figure 2.2 for scenario SSP2-4.5 and the chosen time horizons. Values of HWML are displayed as spatial distribution by constraining parameters of the indicator with the same values used for figure 2.1, to allow comparison. For all time horizons there is an increase in the number of heat wave events and the spatial differences observed in the reference period are accentuated with time. The spatial distribution of indicator anomalies is useful to assess the spatial dependency of indicators, e.g. in figure 2.2 differences between the reference point of the studied system and the are clearly visible. These information can be useful in CCRAs which have a local spatial extension. The main disadvantage is on the study of effects of varying parameters: only a single combination of values can be considered at a time and this limits the visual analysis on the impacts of these values on the indicator.

Aggregate the spatial dimensions

To compress information on spatial dependency, the spatial aggregation is performed by using empirical orthogonal function (EOF) analysis as a dimensionality reduction technique.[7] The following procedure is applied to every

[7]Terminology is varied. Here the eigenvectors, i.e. spatial patterns, are referred to as EOFs and their coefficients, i.e. temporal patterns, are the principal components (PCs). The object containig data is called design matrix with samples, i.e. observations, organised

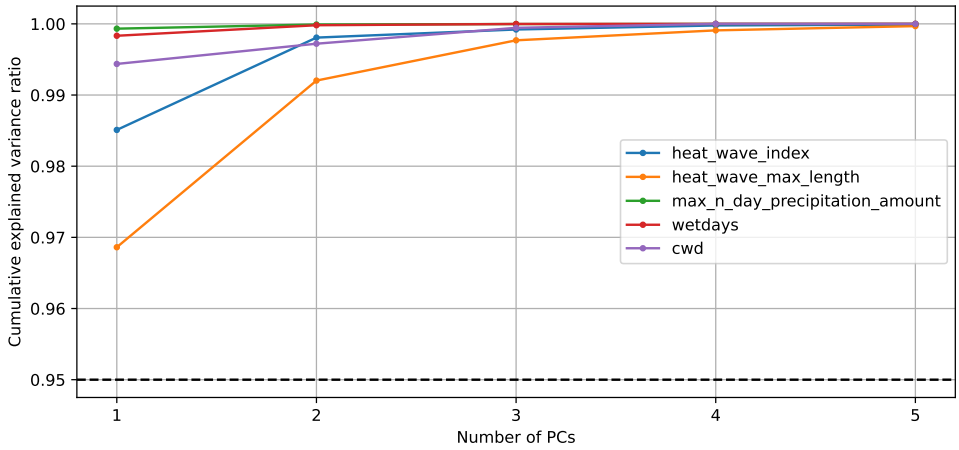

Figure 2.3: Cumulative explained variance resulting from the decomposition in EOFs of all indicators for model EC-Earth3. The dashed line represents the threshold of 95% and only the first five components are displayed for clarity.

indicator I from equation (2.4). First remap the multidimensional array to a bidimensional matrix, i.e. the design matrix, which is needed to perform the EOF analysis. The procedure can be summarised in: assign $S_{\text{lat}} \times S_{\text{lon}}$ as the feature dimension of the design matrix and assign $\prod_{p \in P_I} S_p$ as the sample dimension of the design matrix. This second step establish a bijective relation between the sample dimension of the design matrix and $\prod_{p \in P_I} S_p$, hence each PC effectively maps I to a multidimensional array with coordinates in $\prod_{p \in P_I} S_p$. Then the EOF analysis is applied to the design matrix of the reference period. Data are centred on the sample mean and a spatial weighting considering the curvature of Earth is applied, to avoid losing geographic information [6]: each grid cell is multiplied by $\sqrt{\cos(y)}$ where $y \in S_{\text{lat}}$ is its latitude. Figure 2.3 shows the cumulative explained variance resulting from the EOF analysis of all indicators for model EC-Earth3. A full decomposition is performed but to have plots easier to read it is truncated to the first five PCs. However, the first one collects most of the variance in the sample dimension and this is valid for all models,[8] ensuring that most of the underlying information related to the spatial dimensions are compressed in the first PC.

Vector components of the first two EOFs are shown as spatial fields in figure 2.4 for indicator HWML and model EC-Earth3. This plot shows which features have larger weight in the decomposition, since the first two

in rows and their features, i.e. variables which describe them, in columns. For further clarification on the terminology see [64, pp. 626–627] and for a recap on EOF analysis see [45, pp. 6502–6503] and [34, pp. 1121–1122].

[8] Analogous plots for the other models are available at `https://github.com/mirasac/mscunito-thesis-document/tree/main/figures/torino/indicators/historical/reference/hazard/explained`.

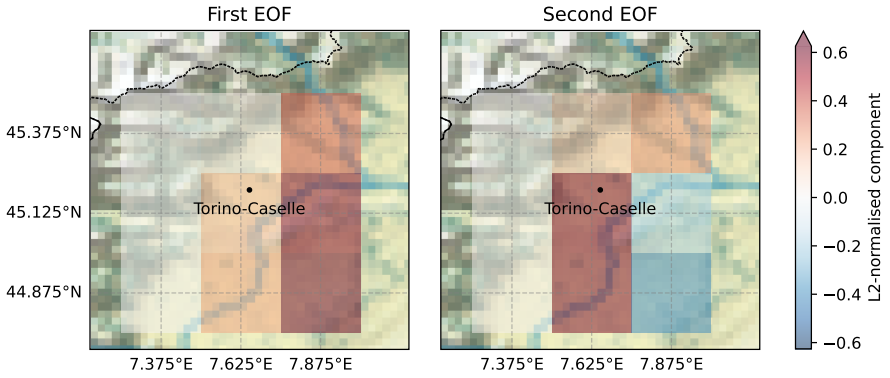

Figure 2.4: First two EOFs of indicator Heat wave max length (symbol HWML, unit day) for model EC-Earth3 in the reference period. Values are normalised with L^2 norm, they are visualised as spatial distribution and represent the weight of each grid cell on the indicator.

PCs together account for the 99% of the total explained variance. Values are normalised with the L^2 norm to compare between various models and indicators. Same normalisation is applied in figure 2.5 where data for each indicator for model EC-Earth3 in the reference period are projected on the first two EOFs.[9] Indicators HWI, HWML and Rxp4day present distribution which are not ascribable to linear correlations, hence other tools may be suitable to study their correlations, e.g. mutual information.

Once the orthogonal basis for the reference period is evaluated, every indicator for the future time horizons is projected on the first vector of the basis. The result is used as new indicator, depending only on its parameters $\underline{z} \in \prod_{p \in P_I} S_p$:

$$I(y, x, \underline{z}) \mapsto I(\underline{z}) \quad . \tag{2.6}$$

The procedure is repeated for each indicator $I \in \mathcal{H}_j$ of each driver j with data from models in each scenario and time horizon.

The projection corresponds to a rotation in the space of all spatial coordinates and this is geometrically possible because feature and sample dimensions are equal for all periods. In fact, parameters obtained from the reference period are used for the indicator in same scenario and model.

The issue of p3 Threshold of tasmin being larger than p2 Threshold of tasmax for some values does not affect the spatial aggregation. This is the result of removing all combinations having the problematic value of p3,

[9]Both plots for other models and indicators are available at `https://github.com/mirasac/mscunito-thesis-document/tree/main/figures/torino/indicators/historical/reference/hazard/EOF` and `https://github.com/mirasac/mscunito-thesis-document/tree/main/figures/torino/indicators/historical/reference/hazard/PC`, respectively.

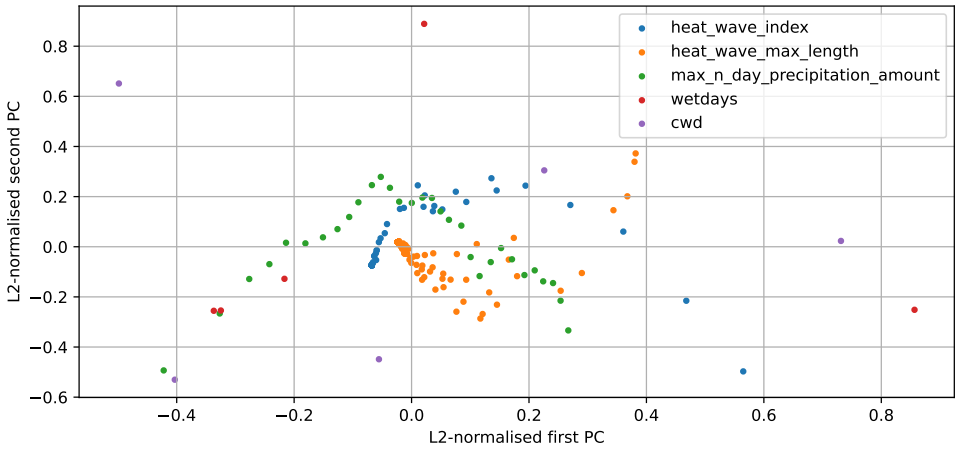

Figure 2.5: First two PCs of indicators for model EC-Earth3 in the reference period of the use case, i.e. from 1st January 1971 to 31st December 2000. Values are normalised with L^2 norm. Non-linear correlations are visible for Heat wave index (symbol HWI), heat wave indicator (symbol HWML) and maximum consecutive p4-day precipitation (symbol Rxp4day).

not only the ones having p3 > p2. The removed coordinates translates in a deletion of rows in the design matrix, effectively reducing the sample dimensions but allowing a rotation without undefined values being involved.

A side effect of the rotation is to possibly obtain negative values which the original indicator was not allowed to get. This is an outcome of the mathematical treatment of quantities and the physical meaning of scalar quantities after the rotation is seldom preserved.

The first EOF is the direction in the feature dimension which maximises the variance among all values of parameters, i.e. the sample dimension. With the procedure for spatial aggregation presented above, the expectation is that higher variance in the space of all parameters corresponds to greater effects on the final risk value. This reasoning extends to the choice of the orthogonal basis: relevant spatial information are gathered in the first EOF of the reference period and the projection on this direction allows to compare the same information in future periods, potentially assessing their change.

On the contrary, applying an EOF analysis to every period and using the first PC, instead of using only the reference period, invalids the comparison of relevant spatial information between different periods. In other words, the direction of maximum variance is not guaranteed to be the same across different periods.

Although it is common to use EOF analysis to decouple the temporal dimension from the spatial ones [34], this procedure is not applied in the present study because each analysed function depends on additional arguments. If spatial aggregation were performed first, either it is applied independently to each combination of parameter values or every dimension which

is not s spatial one is included the sample dimension. In both cases, the resulting indicator would be function $I(t, \underline{z})$, however the resulting orthogonal basis would not allow the comparison between different time horizons. In fact, in the first case there is no guarantee that the direction of maximum variance of the indicator on the sample dimension S_y is the same for every combination of parameter values. In the second case the sample dimension is $S_\mathrm{y} \times \prod_{p \in P_I} S_p$, hence any known interpretation of the results of EOF analysis in terms of time and space is not applicable.

Obtain scalar values for the indicators

To execute module 5, first the scale of each indicator is defined. In this work all indicators are numeric values and may have both metric or categorical scales (i.e. values are distributed uniformly or not, respectively, cf. [59, p. 109]). When metric scales are involved, the methodology suggests to apply the min-max normalisation. Instead, in the present work indicators which are scalar values are not transformed,[10] while indicators which depend on parameters are standardised, i.e. substituted by their z-score. More in detail, for any indicator I undergoing normalisation, the new value is

$$I(\underline{z}) \mapsto I(\underline{z}) = \frac{I(\underline{z}) - \mu_I}{\sigma_I} \tag{2.7}$$

where the sample mean

$$\mu_I = \frac{1}{\prod_{p \in P_I} |S_p|} \sum_{\underline{z} \in \prod_{p \in P_I} S_p} I|_\mathrm{ref}(\underline{z}) \tag{2.8}$$

and the sample standard deviation

$$\sigma_I = \sqrt{\frac{1}{\prod_{p \in P_I} |S_p| - 1} \sum_{\underline{z} \in \prod_{p \in P_I} S_p} \left(I|_\mathrm{ref}(\underline{z}) - \mu_I \right)^2} \tag{2.9}$$

are calculated using values obtained for the reference period $S_\mathrm{y}|_\mathrm{ref}$ [48, p. 84]. Note that the spatial aggregation procedure used above implies that $\mu_I = 0$. The advantage of equation (2.7) with respect to min-max normalisation is to be flexible when new values are introduced, in fact they are measured in terms of statistics of the reference period without breaking the normalisation.[11] To normalise categorical scales, the methodology suggests first to group the values in five classes, then replace them with specific values in the range $[0, 1]$, see [59, pp. 115–116]. Higher normalised values are associated

[10] Formally they are divided by a unitary value of their quantity to obtain dimensionless values, which are trivially compatible and easily used as arguments in mathematical functions.

[11] See section B.1 for further insight on why min-max normalisation is not used.

to more negative impacts. However, this case does not occur in the present study since every indicator with categorical scale is a constant value. Not normalising some indicators may seem wrong since normalisation is a requisite to compare them, but the reason is supported mathematically in the next paragraphs.

For module 6, the weight w_I of each indicator I is set to 1, because no particular influence on the final risk is known a priori. Since indicators are unique, there is not ambiguity to identify their weights with their names as labels. This choice of weighting has not effects on the final risk value, as explained in section 2.3.3. Then, for each determinant the weighted mean of its indicators is computed. Since all indicators are weighted equally, the result equals the arithmetic mean. In [30, p. 51] this process is represented graphically with a single indicator for each driver. The results are a scalar value for exposure

$$E = \frac{1}{\sum_i \sum_{I \in \mathcal{E}_i} w_I} \sum_i \sum_{I \in \mathcal{E}_i} w_I I \quad , \tag{2.10}$$

a scalar value for vulnerability

$$V = \frac{1}{\sum_k \sum_{I \in \mathcal{V}_k} w_I} \sum_k \sum_{I \in \mathcal{V}_k} w_I I \tag{2.11}$$

and a scalar function for hazard $H : \prod_j \prod_{I \in \mathcal{H}_j} \prod_{p \in P_I} S_p \to \mathbb{R}$, which depends on all parameters, defined as

$$H(\underline{z}) = \frac{1}{\sum_j \sum_{I \in \mathcal{H}_j} w_I} \sum_j \sum_{I \in \mathcal{H}_j} w_I I(\underline{z}_I) \tag{2.12}$$

where $\underline{z}_I \in \prod_{p \in P_I} S_p$ is the sequence of values for parameters which are arguments of I. Note that the there is no need to treat drivers of adaptive capacity and sensitivity separately because the aggregation procedure is applied equally to them.

In module 6 a relation between indicators within the same determinant is established through the aggregation procedure, therefore the results may be regarded as category 1 complex hazards. Moreover, the concept of intermediate impact, which mediates drivers of hazard and vulnerability, are a form of category 2 complex hazard [30, p. 33].

2.3.3 Evaluation of risk

Scalar values representing each determinant of risk are aggregated into a single value. The aggregation procedure is a weighted mean, see module 7, and the weights assigned to each determinant are $w_E = 1$, $w_H = 1$ and $w_V = 1$. Then, analogously to the aggregation of hazard indicators in equation 2.12,

the value for risk is a scalar function $R : \prod_j \prod_{I \in \mathcal{H}_j} \prod_{p \in P_I} S_p \to \mathbb{R}$ which depends on all parameters:

$$R(\underline{z}) = \frac{w_E E + w_H H(\underline{z}) + w_V V}{w_E + w_H + w_V} \quad . \tag{2.13}$$

The risk value is a linear function of normalised hazard indicators. This can be seen easily by manipulating equation (2.13),

$$R(\underline{z}) = c_0 + \frac{w_H H(\underline{z})}{w_E + w_H + w_V} = c_0 + c_1 \sum_j \sum_{I \in \mathcal{H}_j} w_I I(\underline{z}_I) \tag{2.14}$$

with $c_0 = \frac{w_E E + w_V V}{w_E + w_H + w_V}$ and $c_1 = \frac{w_H}{(w_E + w_H + w_V) \sum_j \sum_{I \in \mathcal{H}_j} w_I}$, and it holds true as long as the aggregation procedures for risk and hazard are linear.

One of the problems which justifies this work can be stated using equation (2.13): given different choices of indicators or parameters, the resulting risk value can be the same, as long as the differences in values balance out.

Example

Risk is assessed for a system, E and V are known and only one driver of hazard is considered. Two sets of different indicators are prepared, $\mathcal{H}'$ and $\mathcal{H}''$, functions may differ only in the values of their parameters.These alternatives would be equivalent to describe the driver mathematically from different points of view.
Even if all indicators have different values after the calculation steps, the aggregated values of hazard H' and H'' for sets $\mathcal{H}'$ and $\mathcal{H}''$, respectively, are ideally equal. The same same risk value R results from the aggregation, since E and V do not depend on the choices regarding the hazard. This is the expected outcome, because changing the mathematical description of the physical phenomenon should not change the final risk.

The entire pipeline described up to this point spanning sections 2.3.2 and 2.3.3 is repeated for each model available in the ensemble. The outcome is an ensemble of risk values, collected as functions R from equation (2.13) or in the form of multidimensional array. To extract statistical information from these data, an ensemble average is performed to obtain a representative value and the sample standard deviation is associated to it as uncertainty.

However, this procedure poses two issues. The first problem is the disalignment of coordinates in the risk outcome of each model. In other words, the parameters values used as coordinates are not guaranteed to be the same between models. This is consequence of the selection of parameters related to ECVs: even assuming that every model samples from the same distribution of a given ECV, this sample may not be large enough to provide the same

statistics across models, e.g. the quantiles used as values for the interested parameter. To circumvent this problem, in the following the values of these parameters are identified by their quantile order. Parameters affected by this issue are Threshold of tasmax p2, Threshold of tasmin p3 and Threshold of pr p5, as specified in table 2.9. Their values for each model are listed in section A.2, along with their ensemble average and standard deviation, to provide an estimate of practical values to use in CCRAs.

A second issue is the propagation of missing combinations of values in some models. When ensemble average is performed on risk values, the same approach of the temporal aggregation is implemented: models with missing combinations are skipped and the sample is reduced in size from 22 members to 16. The reduction of predictive skill of averages on risk occur only for some combinations of coordinates, namely the ones containing the quantile of order 1.0 of parameter Threshold of tasmin p3 (see table A.2 for the affected models).

A final non-linear transformation is performed on risk value R, to simplify the presentation and comparison of results. Values obtained from all the combinations of parameters are classified accordingly to five categories [30, p. 53], in increasing order of severity:

1. Very low;
2. Low;
3. Intermediate;
4. High;
5. Very high.

This transformation can be formalised as a piecewise function $r : \prod_j \prod_{I \in \mathcal{H}_j} \prod_{p \in P_I} S_p \to \{1, 2, 3, 4, 5\}$, where the thresholds for each piece identify five equally spaces intervals in the set of risk values of the reference period, i.e. the image of $\prod_j \prod_{I \in \mathcal{H}_j} \prod_{p \in P_I} S_p$ through function $R|_{\text{ref}}$:[12]

$$r(\underline{z}) = \begin{cases} \text{Very low} & R(\underline{z}) < q_1 \\ \text{Low} & q_1 \leq R(\underline{z}) < q_2 \\ \text{Intermediate} & q_2 \leq R(\underline{z}) < q_3 \\ \text{High} & q_3 \leq R(\underline{z}) < q_4 \\ \text{Very high} & R(\underline{z}) \geq q_4 \end{cases} . \tag{2.15}$$

Thresholds q_1, q_2, q_3 and q_4 are calculated from risk values of the reference period because hazard drivers are supposed to change risk and impacts with

[12] This is equivalent to apply the min-max normalisation and divide the interval $[0, 1]$ in five parts, as hinted by [31, p. 74].

time. Moreover, the pieces of the function reflect the fact that the image of R is not bounded, due to the aggregated values of determinants being not bounded by the chosen normalisation. This allows to account for extreme values of risk in periods different from the reference.

The underlying idea is that in the past, more precisely in the reference period, any risk and impact was well known and being responded to with proper measures. Any variation with respect to that baseline is worth considering for adaptation and mitigation strategies against negative impacts of climate change.

Finally, module 7 addresses the possible aggregation of multiple sub-risks into an overall risk value [30, p. 54]. According to section 1.1.2, the outcome would be a complex risk belonging to category 3. This additional elaboration is not implemented in the present work because an individual risk is studied, i.e. the climate risk.

2.4 Case study

The methodology of CCRA is applied in particular to Torino-Caselle airport, located near the municipality of Caselle Torinese, in the Metropolitan City of Turin, Italy. The central coordinates for the grid cells are $(45.203° \text{ N}, 7.649° \text{ E})$ in decimal degrees. These data are derived from Ente Nazionale per l'Aviazione Civile (ENAC), the Italian civil aviation authority [24].

The construction of the airport in its modern settings started in 1949 and major upgrades to infrastructures happened before 2006 (see [51, p. 18] for a summary on the history of the airport). Therefore, the reference period is

$$S_{\text{time}}|_{\text{ref}} = \{t : t \text{ day from 1st January 1971 to 31st December 2000}\} \quad . \tag{2.16}$$

For the present CCRA, the airport is considered unaffected by structural changes starting from year 2006. Hence indicators values for that year or closest to it are chosen.

2.4.1 System-dependent data

In section 2.3.1 the reasons behind the selection of indicators are discussed. In this section their values related to Torino-Caselle airport are presented. Values of exposure indicators are shown in table 2.10, values of vulnerability are in table 2.11. The exposure is quantified using data on the operativity of the airport and they are gathered from [65, pp. 154–179].

Same source is used for values of sensitivity. A note on the Age buildings indicator is due: following [19, p. 5], it is the difference in years between the time of writing and the start of the construction of the airport, since

Table 2.10: Values of exposure indicators. The part of the table above the line shows the air-side components, below the line there are the land-side components. Dimensionless quantities have an empy cell in the Unit column.

Indicator	Symbol	Unit	Value
Runways area	e1	m^2	198000
Terminals area	e2	m^2	51150
Offices and other buildings area	e3	m^2	4245
Carparks number	e4		3000

the oldest components are supposed to be the most vulnerable. Because Torino-Caselle airport was subject to various changes, dating back before its designation for civil aviation, the year 1949 is approximated as the starting year for all operations and the lifecycle of the airport components. Instead, structural changes are supposed to end in year 2006, hence the age is evaluated between years 1949 and 2006. This is an heavy approximation because Age buildings is an indicator which directly states the passing of time. However, for the purposes of this study, this level of accuracy is considered acceptable as the focus is not on obtaining precise CCRA results but on assessing how changes in parameters affect those results. A more dynamic CCRA methodology may be an interesting extension of the present study.

Indicators of adaptive capacity are mainly categorical and they are gathered from [51, pp. 66–79]. For use in calculations, categorical values are converted to a numerical scale following [18, p. 6]. The target values are in the interval $[0, 1]$, with lower values indicating lower risk. More in detail, the presence of mitigation or adaptation strategies scores 0.1, while their absence scores 0.9. Intermediate values correspond to the existence of plans that have not yet been implemented. For this reason, the values for the indicators Risk awareness and Guidelines for adaptation plan to climate change are set considering the planning for adaptation and mitigation strategies from the years after 2006.

Table 2.11: Values of vulnerability indicators. Adaptive capacity and sensitivity are above and below the line, respectively. Dimensionless quantities have an empty cell in the Unit column.

Indicator	Symbol	Unit	Value
Risk awareness	v1		0.3
Guidelines for adaptation plan to climate change	v2		0.5
Efficient drainage system	v3		0.1
Monitoring and alarm system	v4		0.9
Bioinfiltration and permeable pavements	v5		0.1
Soil sealing	v6	m^2	2450000
Passengers	v7		3219317
Age buildings	v8		57
Air traffic	v9		53169
Underground infrastructures	v10	m^2	0

Chapter 3

Results and Discussion

3.1 Temporal evolution of risk

Once the CCRA methodology presented in section 2.3 is applied to the Torino-Caselle airport, different risk values are obtained for different combinations of parameters values. Then, the sensitivity of risk on parameters can be assessed. In the following paragraphs the SA is performed with the help of plots and for some possible applications.

The first information that can be drawn is the evolution of risk across the selected time horizons, for a given scenario. Figure 3.3 shows the change of risk for scenario SSP2-4.5 and how varying the Threshold of tasmax p2 affects the outcome. Values of p2 are distributed between 24 °C and 36 °C, see figure 3.1 for an overview on ensemble variability. The remaining parameters are fixed to obtain the bidimensional plots displayed in figure: all values defined by quantiles are set to the 99th percentile, i.e Threshold of tasmin p3 = (19.2 ± 0.4) °C and Threshold of pr p5 = (42 ± 3) mm/day. Instead, the numbers of Consecutive days of extreme temperature p1 = 4 day, to include ranges of consecutive days used in definitions of extreme temperature event, and Consecutive days of extreme precipitation p4 = 5 day, as commonly used in similar indicators, e.g. Rx5day [32, p. 2208]. Quantiles at lower order correspond to lower temperature thresholds in each model, as can be observed qualitatively from figure 3.2. This allows more days each year being classified as heat wave events, therefore increasing the total risk value.

Overall, risk is higher for more distant time horizons, in accordance with the observations and predictions on climate change [40, pp. 8–19]. The standard deviation of risk values increases as well, due to the inter-model differences, decreasing the accuracy on risk prediction.

In the near future, risk values are limited to categories Very low, Low, Intermediate and High. The medium-term future period presents a similar situation, with the exception of the Very high category being compatible only for the lowest value of p2. From the point of view of the analyst,

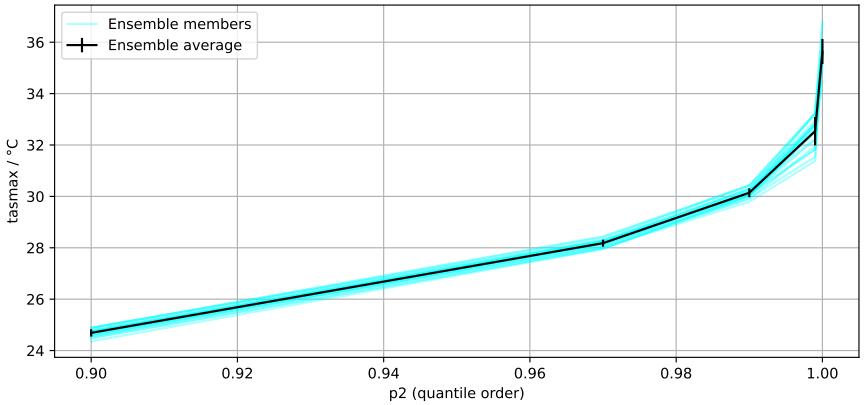

Figure 3.1: Quantiles of tasmax evaluated in the reference period from data of each model. These values are used for parameter p2 Threshold of tasmax during calculations. The ensemble average with standard deviation as estimate of uncertainty is displayed for reference.

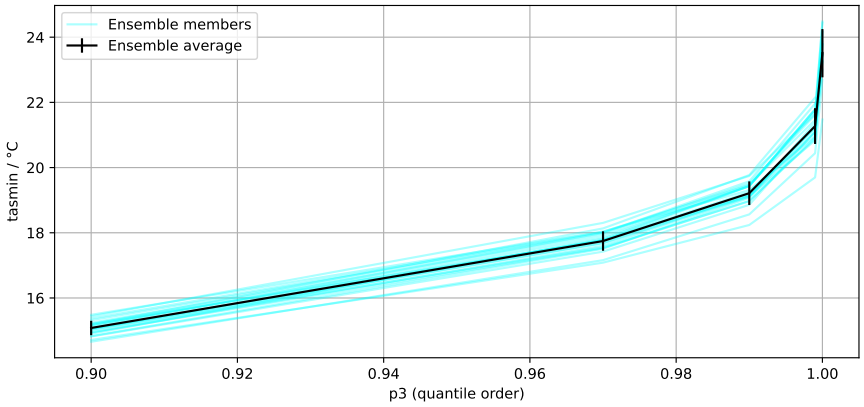

Figure 3.2: Quantiles of tasmin evaluated in the reference period from data of each model. These values are used for parameter p3 Threshold of tasmin during calculations. The ensemble average with standard deviation as estimate of uncertainty is displayed for reference.

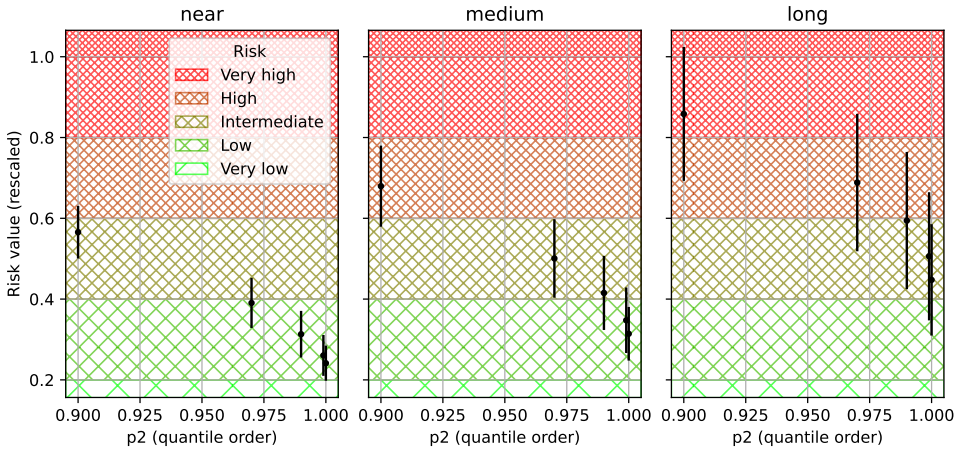

Figure 3.3: Outcome of the CCRA for scenario SSP2-4.5. The threshold of tasmax is varied and the other parameters are fixed to values p1 = 4 day, p4 = 5 day and quantiles of order 0.99 for p3 and p5. The risk value is rescaled with respect to the risk in the reference period from 1st January 1971 to 31st December 2000.

common choices of the threshold between the 90th and the 99th percentiles (i.e. $(15.1 \pm 0.2)\,°C$ and $(19.2 \pm 0.4)\,°C$, respectively) result in negligible differences on the CCRA outcome.

The long-term period has a more severe outcome because the highest category of risk is more frequent, despite the larger uncertainties. In this case, the selection of threshold value is critical, because it results in very different risk categories: the highest risk is reached for thresholds set at $(24.7 \pm 0.1)\,°C$ and selecting a value within a range of 5 °C allows to span up to three categories of risk.

The previous considerations apply for outcomes of scenario SSP3-7.0, see figure 3.4. According to the scenario definition, impacts of climate change are more intense and this is reflected in the long-term period, where threshold values up to 99th quantile result in risk compatible with the highest category.

Risk values for scenario SSP1-2.6 are not affected by climate change, as can be observed in figure 3.5. All values remain constant over time within the standard deviation of the model ensemble, with the only variation between time horizons being an increase in uncertainty. For this scenario, it is reasonable to assume that the threshold value chosen from the reference period data is robust for prediction of risk.

Another threshold which is considered in the present study is for daily precipitation pr. Parameter p5 Threshold of pr affects indicators Rp5mm and CWD, which describe frequency and duration of a heavy precipitation event, respectively (see section 2.3.2). Same considerations of the temperature case above are applied to fix the remaining parameters. Uncertainty on p5 increases for higher order quantiles, as can be seen in figure 3.6, but the effects are negligible with respect to the inter-model variability of risk.

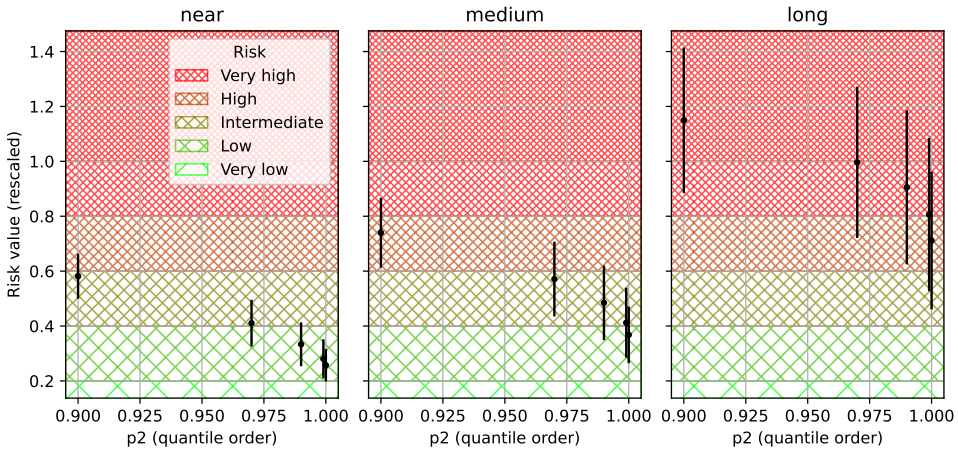

Figure 3.4: Outcome of the CCRA depending on Threshold of tasmax for scenario SSP3-7.0. Same settings of figure 3.3 apply. The risk value is rescaled with respect to the risk in the reference period from 1st January 1971 to 31st December 2000.

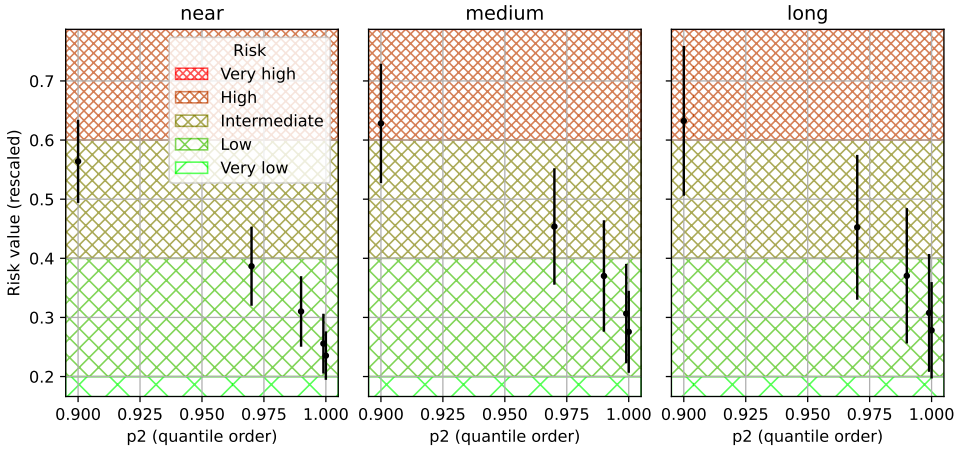

Figure 3.5: Risk resulting from the CCRA as a function of the Threshold of tasmax for scenario SSP1-2.6. Same settings of figure 3.3 apply. The risk value is rescaled with respect to the risk in the reference period from 1st January 1971 to 31st December 2000.

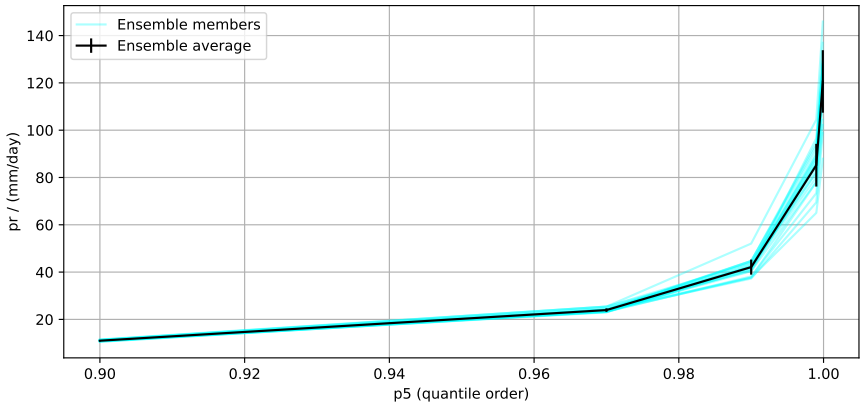

Figure 3.6: Quantiles of pr evaluated in the reference period from data of each model. These values are used for parameter p5 Threshold of pr during calculations. The ensemble average with standard deviation as estimate of uncertainty is displayed for reference.

A proper UA which account for the propagation of uncertainties would be more effective to assess the precision of the CCRA.

Effects of changing scenario are analogous to the temperature case. A difference can be noted in the variability of risk values with respect to threshold values, being smaller than the temperature case, particularly on the long-term horizon. Figure 3.7 show these results for scenario SSP2-4.5.[1]

3.2 Optimal number of consecutive days

The SA of risk dependent on different values of indicator parameters could be useful to study possible improvements to the CCRA methodology currently adopted. In this study a potential application is for the choice of the number of consecutive days, which could be selected objectively instead of adopting any heuristic.

Indicators which depend on the number of consecutive days to define the event they quantify are HWI, HWML and Rxp4day. More in detail, the involved parameters are p1 for heat wave events and p4 for heavy precipitation events. These two parameters are not supposed to have the same value, since they describe different phenomena. However, a relation can be drawn by observing the plot of risk with respect to these parameters.

In figure 3.8 the risk values for scenario SSP2-4.5 are plotted against parameter p1. Every other parameter is fixed to the 99th percentile, which correspond to: Threshold of tasmax p2 $= (30.1 \pm 0.2)\,^{\circ}\mathrm{C}$, Threshold of

[1] See figures `https://github.com/mirasac/mscunito-thesis-document/blob/main/figures/torino/indicators/ssp126/risk/wetdays_thresh-cwd_thresh.pdf` and `https://github.com/mirasac/mscunito-thesis-document/blob/main/figures/torino/indicators/ssp370/risk/wetdays_thresh-cwd_thresh.pdf` for results of scenarios SSP1-2.6 and SSP3-7.0, respectively.

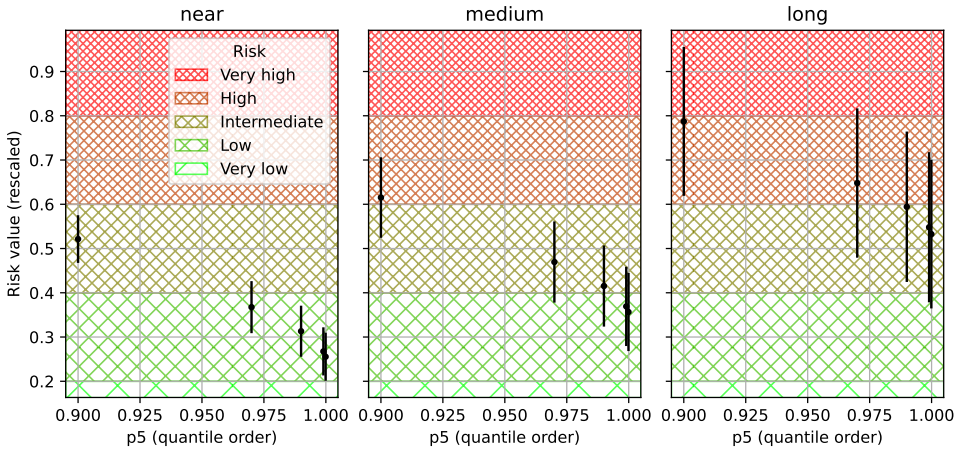

Figure 3.7: Outcome of the CCRA for scenario SSP2-4.5 varying the Threshold of pr. Other parameters are fixed to values p1 = 4 day, p4 = 5 day and quantiles of order 0.99 for p3 and p2. The risk value is rescaled with respect to the risk in the reference period from 1st January 1971 to 31st December 2000.

tasmin p3 = $(19.2 \pm 0.4)\,°C$ and Threshold of pr p5 = (42 ± 3) mm/day. A decreasing trend can be observed, coherent with the intuition that it is more rare to have p1 consecutive days satisfying the selected temperature ranges when it increases in size. Due to the average increase of temperatures with time, risk values in the long-term horizon are larger than the ones in the near-term horizon. From a practical point of view, a common choice of number of Consecutive days of extreme heat p1 < 7 day makes the risk values highly sensible to the time horizon. Therefore, choosing the right value for p1 based on the periods under study becomes important to avoid outcomes dominated by uncertainty.

On the other hand, the curve of risk for precipitation events is increasing, as can be observed in figure 3.9 for scenario SSP2-4.5. Similarly to the temperature case, remaining parameters are set to the 99th percentile to obtain a bidimensional plot. Indicator Rxp4day searched the maximum of pr in samples of p4 days, hence if the parameter is increased, the probability to find a larger value increases as well. These effects are accentuated with time, having larger risk values compatible with the Very high category.

The opposite trends of these plots may suggest the presence of an optimum on the multidimensional surface of the risk function. Further insights are obtained by the joint plot of risk with respect to p1 and p4. To simplify the visualisation of data, future time horizons are analysed one at a time, while to guarantee the comparison with the previous results, remaining parameters are set with the same constraints. In figure 3.10 the 3D plot for scenario SSP2-4.5 and the medium-term horizon is shown. The plot confirms the direction of increment observed in figures 3.8 and 3.9 and does not show a local minimum in the selected domain of parameters. However, by

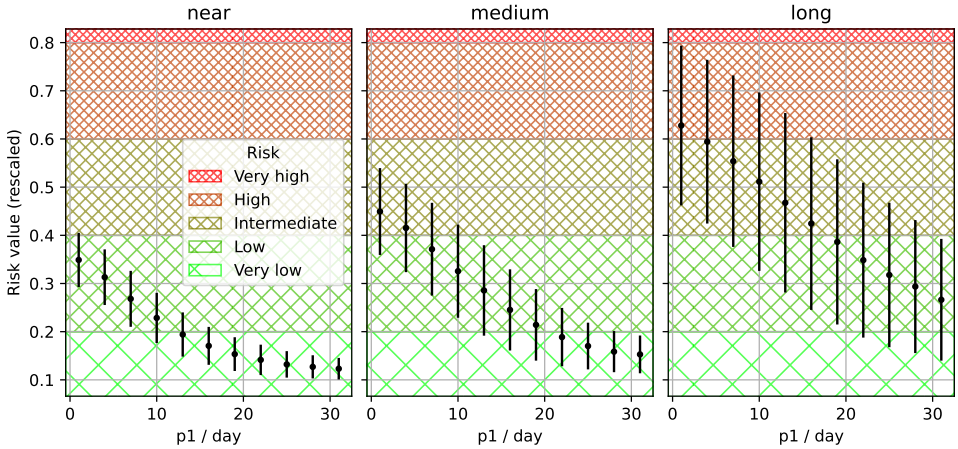

Figure 3.8: Risk values depending on number of consecutive days of extreme heat in scenario SSP2-4.5. Both indicators Heat wave index and Heat wave max length depend on this parameter. Other parameters are set to the percentile of order 0.99. The risk value is rescaled with respect to the risk in the reference period from 1st January 1971 to 31st December 2000.

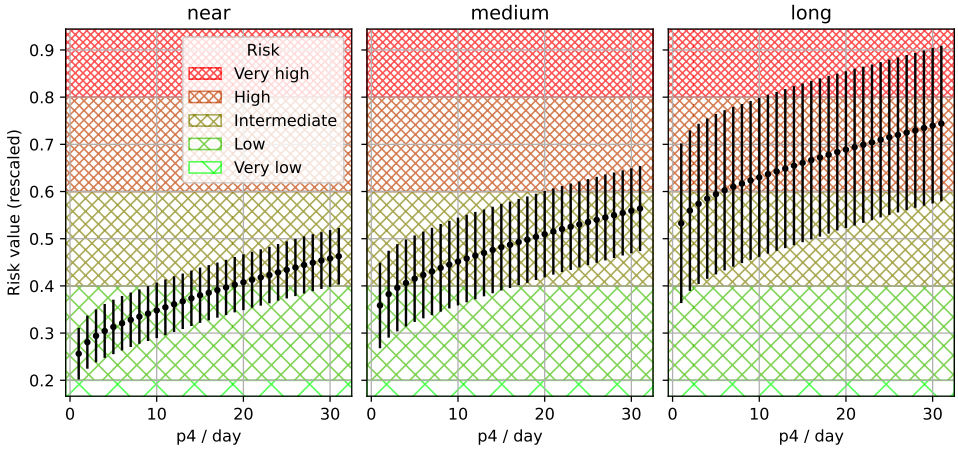

Figure 3.9: Risk values depending on number of consecutive days of extreme precipitation in scenario SSP2-4.5. Other parameters are set to the percentile of order 0.99. The risk value is rescaled with respect to the risk in the reference period from 1st January 1971 to 31st December 2000.

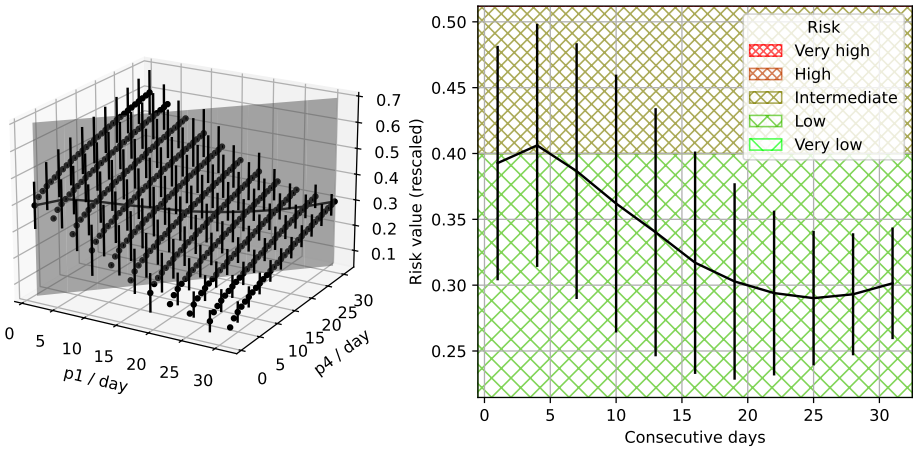

Figure 3.10: Risk values depending on Number of consecutive days of extreme precipitation p4 and Number of consecutive days of extreme temperature p1 in scenario SSP2-4.5 and medium-term horizon. Other parameters are set to the percentile of order 0.99: Threshold of tasmax p2 = $(30.1 \pm 0.2)\,^{\circ}\mathrm{C}$, Threshold of tasmin p3 = $(19.2 \pm 0.4)\,^{\circ}\mathrm{C}$ and Threshold of pr p5 = $(42 \pm 3)\,\mathrm{mm/day}$. The risk value is rescaled with respect to the risk in the reference period from 1st January 1971 to 31st December 2000. The grey vertical plane in the 3D plot represent the constraint on the same values of p1 and p4. Data projected on this plane are displayed with the error bars and the risk categories on the 2D plot.

intersecting with the plane formed by the same values of parameters, two extreme values can be identified. This constraint is equivalent to use the same number of successive days to define both heat wave and heavy precipitation events, which may be an useful choice to streamline the CCRA.

As observed from the bidimensional projections of the risk surface, the maximum is placed at low values of consecutive days, because it represents the highest effects on risk brought by indicators HWI, HWML and Rxp4day combined. For reference, 5 day is the time span suggested for Rxp4day, while temperature-related indicators normally use 6 day [32, p. 2208]. Precise values for the optimal number of consecutive days can not be obtained in the present analysis due to the coarser interval S_{p1} for parameter p1. In fact, the point of maximum would become 4 day but there is no information on neighbour values, which could be compatible with the suggestions from literature instead. A further application of the study with denser intervals is needed to identify the optima more precisely.

On the other hand, the constrasting effects of increasing heavy precipitation events and decreasing heat wave events place the minimum to higher parameter values. For this reason, it can be associated with most extreme events, e.g. heat waves with a length of 25 day for the case presented in figure 3.10. This value could be used in CCRA where the risk associated to combined extreme events regarding temperature and precipitation is studied, with the precondition to set the other parameters to suitable values.

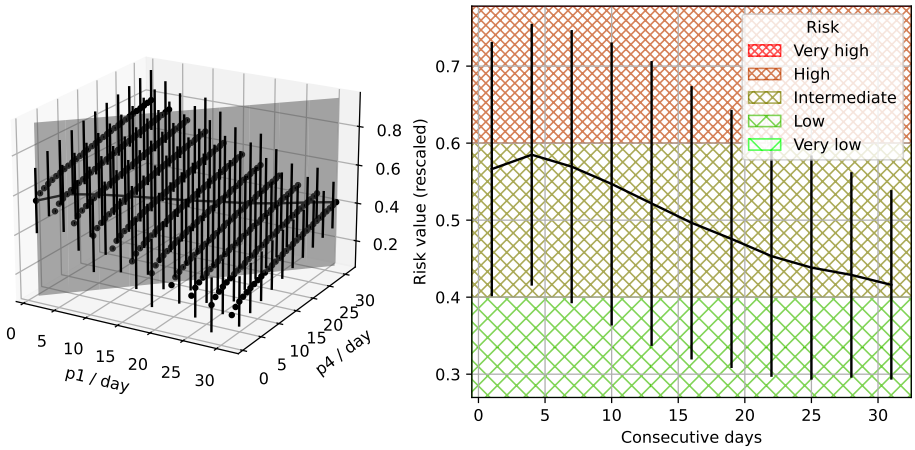

Figure 3.11: Risk values for scenario SSP2-4.5 and Long time horizon. Same settings of figure 3.10 apply.

The optimal values discussed above are not guaranteed to exists in different periods, as can be seen in figure 3.11 for the Long future period, where the minimum is not present in the considered domain of values. Extending the domain of the parameters could recover the missing optimum, but the validity of this operation is subject to context and scope of the CCRA performed, since the explored parameter values could not be useful. In the near-term horizon the minimum is present and associated to lower numbers of consecutive days with respect to the medium-term period, see figure 3.12. This can be explained with the low number of heat wave events present in the near-term horizon, which lowers the risk curve as seen in figure 3.8, therefore reducing the value of the intersection in the 3D plot. The maxima are equal for all future periods, however they bring different risk outcomes.

Scenarios SSP1-2.6 and SSP3-7.0 provides similar results, with risk values which are reduced or amplified due to climate change. Plots are available in files `window_near.pdf`, `window_medium.pdf` and `window_long.pdf` for Near, Medium and Long periods, respectively, at `https://github.com/mirasac/mscunito-thesis-document/tree/main/figures/torino/indicators/ssp126/risk` for scenario SSP1-2.6 and at `https://github.com/mirasac/mscunito-thesis-document/tree/main/figures/torino/indicators/ssp370/risk` for scenario SSP3-7.0.

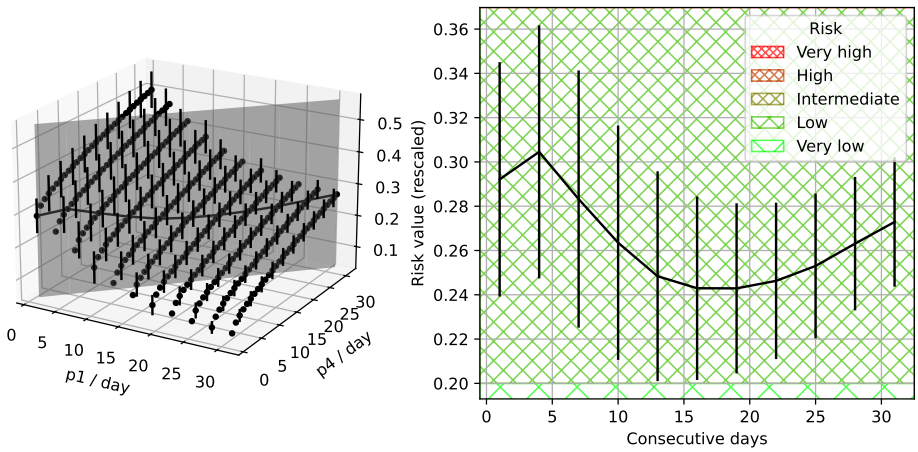

Figure 3.12: Risk values for scenario SSP2-4.5 and Near time horizon. Same settings of figure 3.10 apply.

Chapter 4

Conclusions

The concept of risk is a powerful tool to manage undesired outcomes and cope with an uncertain future. Climate change is one of the main source of risk for the present and future of ecosystems and human activities. Acting ahead of time by understanding the possible impacts of climate change and exploring viable response actions to it is becoming fundamental. Indeed, this is the purpose of climate change risk assessment, which collects information from various stakeholders and involved parties to address to risks generated by climate change and which may affect any valuable system.

Operatively, a climate change risk assessment quantifies risk from climate change, mixing climate data and available information on the system and at various time periods. The ways used to combine data depend on the chosen methodology, and over the years, several variants have emerged from different industries, organisations, and political entities. This variability is a direct consequence of the extent of the concept of risk and related fields. One of the drawbacks of such richness of materials is the lack of a uniform, standardised approach to its application. This is transposed to climate-related fields and climate change risk assessment, where different methodologies suggest different implementations, hampering the possibility to perform a fair comparison between them or a robust procedure to translate the results.

In the present work a methodology of climate change risk assessment is chosen and applied to a system taken as a case study. The methodology includes the most recent interpretation of climate risk, intended as a function of hazard from climate change and vulnerability and exposure of the analysed system. Each of them is a determinant of risk and their purpose is to describe various aspects of the risk studied and the system that can be impacted. Determinants are quantified functions called indicators, in particular the hazard indicators being functions of climate data and additional parameters. The objective of the thesis is to study how variations of parameters values affect the outcome of the climate change risk assessment. An airport is chosen as system under study.

Climate data from the past are used to build a reference for discussing risk in the future. Reanalyses from ERA5 are used as the reference to adjust the bias of the model projection dataset NEX-GDDP-CMIP6. Three different SSP scenarios from ScenarioMIP are used to increase the variability of the outcomes and the final risk values are the averages over an ensemble of 22 CMIP6 models. Then the methodology of risk assessment is followed to identify system-dependent data and relevant indicators. The present work is restricted to two known sources of climate risk: heat wave and heavy precipitation. Indicators from literature are chosen and generalised to allow the variation of parameters they depend on. Both risks and indicators are selected to be meaningful for the application of the methodology to the case study.

Results of the study is risk as a function of parameters in hazard indicators. Risk values are compared across time horizons and related to the risk of the reference period.

Plots generated for some indicators show the temporal evolution of risk and the differences across scenarios, which are coherent with their description of future climate change. Generally a climate change risk assessment as a limited spatial extension and the information related to the system are limited in time, depending on the context and scope of the assessment. Observations carried out in the first result suggest that parameters for hazard indicators should be adapted to time horizons, to avoid excessive or meaningless risk values resulting from the assessment.

The multidimensional aspect of resulting data is leveraged to propose a procedure of selection of the number of consecutive days, which is a parameter in indicators of both temperature and precipitation. When the relevant indicators are included in the same climate change risk assessment, this procedure provides a rule to select univocally a parameter value, depending on the period of interest.

The present work tries to quantify some weaknesses of existent methodologies of climate change risk assessment with the support of computational tools. The procedures adopted here could be tested on other different case studies and for more specific characterisations of climate risk, to provide and improve robust practical tools at each iteration. A uniform but flexible framework for climate change risk assessment may seems unreachable, but as tiny steps as the present work may help to reduce the gap.

Appendix A

Additional implementation details

A.1 Selection of CMIP6 models

Some models available in NEX-GDDP-CMIP6 are excluded from the present study because they present issues which can not be contained without affecting the calculation. Table A.1 list both the used models and the excluded models, along with additional information.

The most frequent issue is the lack of data for some of the used ECVs or for some SSPs. On the contrary, model GISS-E2-1-G occasionally presents multiple values for the same day, hence to avoid introducing systematic errors on which values should be considered or how to aggregate them, the model is excluded from the list.

Finally, two models have temporal coordinates set on a different calendar than the one used in this work, namely a 360-day calendar. Calendars are defined by the Model Intercomparison Project (MIP) endorsed GCMs but no restriction is imposed on the possibility to convert from one to another.

A.2 Values of parameters defined by quantiles

Calculations presented in section 2.3 are performed separately for each model. This procedure has the advantage to propagate information related to the specific models throughout the methodology and to extract ensemble statistics on the final risk values. However, it makes difficult to track the actual values of parameters based on quantiles, e.g. thresholds on temperature, because they are evaluated on data of the reference period, which in principle are different for each model. Using the order of quantiles resolves the issue of tracking quantities but hinders the interpretation of plots.

To give a reference for quantiles used in the document, they are mapped to their order in plots. One line for every model is drawn to show their vari-

Table A.1: Models available in NEX-GDDP-CMIP6. The part of the table above the line shows the models used in the present study, their CMIP6 variant is specified. Below the line the models which are excluded are listed, along with the reason for their exclusion.

Model	Notes
ACCESS-CM2	Variant r1i1p1f1
ACCESS-ESM1-5	Variant r1i1p1f1
BCC-CSM2-MR	Variant r1i1p1f1
CanESM5	Variant r1i1p1f1
CMCC-ESM2	Variant r1i1p1f1
CNRM-CM6-1	Variant r1i1p1f2
CNRM-ESM2-1	Variant r1i1p1f2
EC-Earth3	Variant r1i1p1f1
EC-Earth3-Veg-LR	Variant r1i1p1f1
FGOALS-g3	Variant r3i1p1f1
GFDL-ESM4	Variant r1i1p1f1
INM-CM4-8	Variant r1i1p1f1
INM-CM5-0	Variant r1i1p1f1
IPSL-CM6A-LR	Variant r1i1p1f1
MIROC-ES2L	Variant r1i1p1f2
MIROC6	Variant r1i1p1f1
MPI-ESM1-2-HR	Variant r1i1p1f1
MPI-ESM1-2-LR	Variant r1i1p1f1
MRI-ESM2-0	Variant r1i1p1f1
NorESM2-LM	Variant r1i1p1f1
NorESM2-MM	Variant r1i1p1f1
TaiESM1	Variant r1i1p1f1
CESM2	Missing data
CESM2-WACCM	Missing data
CMCC-CM2-SR5	Missing data
GFDL-CM4	Missing data
GFDL-CM4_gr2	Missing data
GISS-E2-1-G	Data with sub-daily resolution
HadGEM3-GC31-LL	Missing data
HadGEM3-GC31-MM	Missing data
IITM-ESM	Missing data
KACE-1-0-G	Calendar of 360 days
KIOST-ESM	Missing data
NESM3	Missing data
UKESM1-0-LL	Calendar of 360 days

Table A.2: Quantiles of parameter p2 Threshold of tasmax for each model used in the evaluation of indicators. Ensemble average and standard deviation are shown at the bottom of the table.

Model	Order 0.9 °C	Order 0.97 °C	Order 0.99 °C	Order 0.999 °C	Order 1.0 °C
ACCESS-CM2	24.6	28.2	30.0	32.2	35.5
ACCESS-ESM1-5	24.6	28.0	30.0	32.5	34.5
BCC-CSM2-MR	24.9	28.4	30.4	33.3	36.1
CanESM5	24.8	28.2	30.1	32.8	35.8
CMCC-ESM2	24.8	28.2	30.2	32.6	35.2
CNRM-CM6-1	24.9	28.3	30.4	33.2	36.7
CNRM-ESM2-1	24.7	28.1	30.1	33.2	36.8
EC-Earth3	24.7	28.0	29.8	31.4	35.9
EC-Earth3-Veg-LR	24.7	28.1	29.9	32.0	35.5
FGOALS-g3	24.7	28.2	30.1	32.8	35.9
GFDL-ESM4	24.5	28.0	29.9	31.5	35.4
INM-CM4-8	24.9	28.4	30.4	32.8	35.6
INM-CM5-0	24.5	28.0	30.0	32.5	35.4
IPSL-CM6A-LR	24.8	28.3	30.2	32.2	35.0
MIROC-ES2L	24.4	27.9	30.0	32.8	35.6
MIROC6	24.6	28.1	30.2	32.8	35.6
MPI-ESM1-2-HR	24.5	28.2	30.1	32.7	35.6
MPI-ESM1-2-LR	24.9	28.3	30.3	33.2	35.8
MRI-ESM2-0	24.7	28.2	30.3	32.6	35.6
NorESM2-LM	24.7	28.3	30.3	32.9	35.5
NorESM2-MM	24.6	28.2	30.1	31.8	35.5
TaiESM1	24.7	28.3	30.0	31.8	35.5
Mean	24.7	28.2	30.1	32.5	35.6
Standard deviation	0.1	0.1	0.2	0.6	0.5

ability in the ensemble, but no reference to the particular models is made because their comparison is beyond the purpose of this work. Points for the ensemble average and error bars representing the uncertainty estimated through standard deviation are overlapped in the same plot. Figures 3.1 and 3.2 show quantiles of tasmax and tasmin, respectively, while figure 3.6 shows quantiles of pr. Raw values are available in CSV format at `https://github.com/mirasac/mscunito-thesis-code/tree/main/data/torino/indicators/historical/reference/parameters`, but they are displayed with associated uncertainty given by the standard deviation in tables A.3, A.2 and A.4 for easier access.

Table A.3: Quantiles of parameter p3 Threshold of tasmin for each model used in the evaluation of indicators. Ensemble average and standard deviation are shown at the bottom of the table. Missing values are identified with NA and are skipped during the evaluation of statistics, hence reducing the sample size and the predictive skill of the estimators.

Model	Order 0.9 °C	Order 0.97 °C	Order 0.99 °C	Order 0.999 °C	Order 1.0 °C
ACCESS-CM2	14.9	17.5	19.0	20.9	23.4
ACCESS-ESM1-5	15.2	17.8	19.2	21.2	23.3
BCC-CSM2-MR	15.0	17.6	19.0	20.9	23.3
CanESM5	15.4	18.3	19.7	21.6	24.5
CMCC-ESM2	15.2	17.9	19.4	21.7	24.2
CNRM-CM6-1	15.5	18.0	19.3	21.0	23.2
CNRM-ESM2-1	15.2	17.8	19.1	20.8	23.8
EC-Earth3	15.3	18.0	19.5	21.6	NA
EC-Earth3-Veg-LR	15.2	17.9	19.4	21.8	NA
FGOALS-g3	15.0	17.6	19.1	21.3	23.5
GFDL-ESM4	14.9	17.8	19.4	21.8	24.4
INM-CM4-8	15.1	17.8	19.4	21.8	NA
INM-CM5-0	14.8	17.4	18.9	21.1	23.9
IPSL-CM6A-LR	15.4	18.0	19.5	21.5	24.2
MIROC-ES2L	14.7	17.2	18.6	20.4	22.7
MIROC6	14.7	17.1	18.2	19.7	21.5
MPI-ESM1-2-HR	15.0	17.7	19.2	21.2	23.5
MPI-ESM1-2-LR	15.1	17.7	19.1	21.1	23.0
MRI-ESM2-0	15.2	18.1	19.8	22.1	NA
NorESM2-LM	15.1	18.0	19.6	22.0	NA
NorESM2-MM	15.1	17.8	19.2	21.1	NA
TaiESM1	14.8	17.5	19.1	21.4	23.8
Mean	15.1	17.7	19.2	21.3	23.5
Standard deviation	0.2	0.3	0.4	0.5	0.7

Table A.4: Quantiles of parameter p5 Threshold of pr for each model used in the evaluation of indicators. Ensemble average and standard deviation are shown at the bottom of the table.

Model	Order 0.9 mm/day	Order 0.97 mm/day	Order 0.99 mm/day	Order 0.999 mm/day	Order 0.9999 mm/day
ACCESS-CM2	10.9	23.5	42	80	100
ACCESS-ESM1-5	11.3	23.4	38	78	120
BCC-CSM2-MR	11.0	24.3	45	94	130
CanESM5	11.0	24.2	43	82	110
CMCC-ESM2	11.2	24.2	42	82	120
CNRM-CM6-1	10.9	23.9	45	92	130
CNRM-ESM2-1	10.8	23.8	45	95	130
EC-Earth3	11.4	24.8	41	78	110
EC-Earth3-Veg-LR	10.9	23.9	37	70	100
FGOALS-g3	10.8	23.6	42	86	130
GFDL-ESM4	11.0	24.1	44	86	120
INM-CM4-8	10.7	23.5	40	86	120
INM-CM5-0	11.0	24.1	38	65	90
IPSL-CM6A-LR	11.3	25.4	44	88	120
MIROC-ES2L	10.9	23.2	41	87	130
MIROC6	10.6	23.2	38	73	100
MPI-ESM1-2-HR	11.2	25.4	42	84	120
MPI-ESM1-2-LR	11.2	23.4	41	88	120
MRI-ESM2-0	11.5	25.4	52	105	150
NorESM2-LM	10.8	23.0	42	97	140
NorESM2-MM	10.5	23.4	43	90	130
TaiESM1	10.8	23.1	42	90	130
Mean	11.0	23.9	42	85	120
Standard deviation	0.3	0.8	3	9	10

Appendix B

Mathematical considerations

B.1 Min-max normalisation

When min-max normalisation is applied to a given indicator, it is rescaled to the $[0, 1]$ interval, with higher values associated to more negative impacts. If multiple temporal periods are involved, one is chosen as reference for the extreme values [48, p. 85].

There is the implicit assumption is that the image of the indicator is bounded and its extremes are known. This is not always true, hence the extremes must be set in alternative ways (e.g. by discussing with experts, by consulting the literature, by analysing the system), see [59, pp. 113–115].

Once the extremes are found, the min-max normalisation of an indicator can be evaluated easily. Denote its image as $X \subset \mathbb{R}$ and the extremes as $x_{\max} = \max X$ and $x_{\min} = \min X$. Then the min-max normalisation applied to $x \in X$ is

$$\frac{x - x_{\min}}{x_{\max} - x_{\min}} \quad . \tag{B.1}$$

In literature the min-max normalisation is frequently applied as suggested by the methodology (cf. [17, p. 6], [18, p. 6] and [31, p. 74]). In the present work it is not chosen because of two downsides:

1. The methodology is applied to a single system and the ranges of indicators are not known. This means that a single value representing the system exists for any given indicator and trivially it corresponds to its minimum and maximum values, making the outcome of the normalisation undefined. In literature this problem is avoided by considering a set of systems, which results in an ensemble of values for each indicator which is assumed to be its image.

2. In periods different from the reference there may be values of the indicator which exceed the extremes. They result in normalised values

which fall outside the interval $[0, 1]$, invalidating the purpose of the normalisation. In literature this is issue is solved by clipping the exceeding values to the corresponding extremes of the interval.

B.2 Alternative aggregation for risk

Some methodologies suggest to evaluate risk as product of the aggregated values of exposure, hazard and vulnerability:

$$R = E\,H\,V \quad . \tag{B.2}$$

This procedure is used in contexts preceding the concept of risk introduced in [29] and it is still used in later articles (see [17, p. 7] and [18, p. 6]).

This procedure is used because it admits a null risk value, i.e. negligible impacts, when either of the values for its determinant is null. This reasoning is intuitive, but hides the request that values for determinants have exactly value zero when their impacts are negligible or balance out, which depends on the aggregation procedure used to evaluate them from their indicators. Moreover, it neglects the possibility to weight each determinant differently.

With respect to how risk is evaluated in the present work (see section 2.3.3 and equation (B.2)), two considerations can be made on this procedure. First, it is possible to rewrite equation (2.13) as equation (B.2) through a continuous transformation,

$$\begin{aligned} R'(\underline{z}) &= \exp\big(R(\underline{z})\big) = \\ &= \exp\left(\frac{w_E E}{w_E + w_H + w_V}\right) \exp\left(\frac{w_H H(\underline{z})}{w_E + w_H + w_V}\right) \exp\left(\frac{w_V V}{w_E + w_H + w_V}\right) = \\ &= E'\,H'(\underline{z})\,V' \quad . \end{aligned} \tag{B.3}$$

This allows to apply the considerations of the present study to CCRAs which evaluate risk as in equation (B.2). Note that an exact value of $R'(\underline{z}) = 0$ can not be obtained if real data and functions are used in the methodology. Second, in equation (B.2) R is linear with respect to H. As a consequence, if equation (B.2) is used instead of equation (2.13) and every other detail of the methodology follows section 2.3.3, then the risk value R is still a linear function of normalised hazard indicators:

$$R(\underline{z}) = E\,V \sum_j \sum_{I \in \mathcal{H}_j} w_I I(\underline{z}_I) \quad . \tag{B.4}$$

Bibliography

[1] World Meteorological Organization (WMO). *Guidelines on the Definition and Characterization of Extreme Weather and Climate Events*. 2023rd ed. WMO-No. 1310. Geneva: WMO, 2023. 36 pp. ISBN: 978-92-63-11310-8. URL: https://library.wmo.int/idurl/4/58396 (visited on 09/23/2024).

[2] World Meteorological Organization (WMO). *Outcomes of the 2020 Survey on the Impacts of Climate Change and Variability on Aviation*. AeM SERIES 6. Geneva: WMO, 2020. 46 pp. URL: https://library.wmo.int/idurl/4/57199 (visited on 09/23/2024).

[3] World Meteorological Organization (WMO). *WMO Guidelines on the Calculation of Climate Normals*. WMO-No 1203. Geneva: WMO, 2017. ISBN: 978-92-63-11203-3.

[4] World Meteorological Organization (WMO) et al. *The 2022 GCOS Implementation Plan*. 244. Geneva: WMO, 2022, p. 98. URL: https://library.wmo.int/idurl/4/58104 (visited on 09/05/2024).

[5] 14:00-17:00. *ISO 31000:2018*. URL: https://www.iso.org/standard/65694.html (visited on 07/05/2024).

[6] Mark P. Baldwin, David B. Stephenson, and Ian T. Jolliffe. "Spatial Weighting and Iterative Projection Methods for EOFs". In: (Jan. 15, 2009). DOI: 10.1175/2008JCLI2147.1. URL: https://journals.ametsoc.org/view/journals/clim/22/2/2008jcli2147.1.xml (visited on 09/28/2024).

[7] Rawshan Ara Begum et al. "Point of Departure and Key Concepts". In: *Climate Change 2022: Impacts, Adaptation and Vulnerability. Contribution of Working Group II to the Sixth Assessment Report of the Intergovernmental Panel on Climate Change*. Ed. by Hans-Otto Pörtner et al. Cambridge University Press, 2022.

[8] Stephan Bojinski et al. "The Concept of Essential Climate Variables in Support of Climate Research, Applications, and Policy". In: *Bulletin of the American Meteorological Society* 95.9 (Sept. 1, 2014), pp. 1431–1443. ISSN: 0003-0007, 1520-0477. DOI: 10.1175/BAMS-D-13-00047.1.

URL: https://journals.ametsoc.org/view/journals/bams/95/9/bams-d-13-00047.1.xml (visited on 05/11/2024).

[9] Pascal Bourgault et al. "Xclim: Xarray-Based Climate Data Analytics". In: *Journal of Open Source Software* 8.85 (May 18, 2023), p. 5415. ISSN: 2475-9066. DOI: 10.21105/joss.05415. URL: https://joss.theoj.org/papers/10.21105/joss.05415 (visited on 06/08/2024).

[10] Paul Bowyer et al. *Adapting to Climate Change: Methods and Tools for Climate Risk Management*. 17. Climate Service Center, Germany, 2014, p. 124. URL: https://www.climate-service-center.de/about/news_and_events/news/063446/index.php.en (visited on 07/05/2024).

[11] Rachel Burbidge. "Adapting European Airports to a Changing Climate". In: *Transportation Research Procedia*. Transport Research Arena TRA2016 14 (Jan. 1, 2016), pp. 14–23. ISSN: 2352-1465. DOI: 10.1016/j.trpro.2016.05.036. URL: https://www.sciencedirect.com/science/article/pii/S2352146516300369 (visited on 09/23/2024).

[12] Alex J. Cannon, Stephen R. Sobie, and Trevor Q. Murdock. "Bias Correction of GCM Precipitation by Quantile Mapping: How Well Do Methods Preserve Changes in Quantiles and Extremes?" In: (Sept. 1, 2015). DOI: 10.1175/JCLI-D-14-00754.1. URL: https://journals.ametsoc.org/view/journals/clim/28/17/jcli-d-14-00754.1.xml (visited on 09/13/2024).

[13] David Carlin et al. *2024 Climate Risk Landscape Report*. Geneva: UNEP FI, Apr. 2024. URL: https://www.unepfi.org/themes/climate-change/2024-climate-risk-landscape/ (visited on 04/09/2024).

[14] David Carlin et al. *The 2023 Climate Risk Landscape*. UNEP FI, Mar. 2023. URL: https://www.unepfi.org/themes/climate-change/2023-climate-risk-landscape/ (visited on 04/09/2024).

[15] Peter F. Christoffersen. *Elements of Financial Risk Management | ScienceDirect*. 2004. URL: https://www.sciencedirect.com/book/9780121742324/elements-of-financial-risk-management (visited on 08/20/2024).

[16] *Commission Delegated Regulation (EU) 2021/2139 of 4 June 2021 Supplementing Regulation (EU) 2020/852 of the European Parliament and of the Council by Establishing the Technical Screening Criteria for Determining the Conditions under Which an Economic Activity Qualifies as Contributing Substantially to Climate Change Mitigation or Climate Change Adaptation and for Determining Whether That Economic Activity Causes No Significant Harm to Any of the Other Environmental Objectives (Text with EEA Relevance)Text with EEA Rel-*

evance. Jan. 1, 2024. URL: http://data.europa.eu/eli/reg_del/2021/2139/2024-01-01/eng (visited on 04/23/2024).

[17] Carmela De Vivo et al. "Application of Climate Risk Assessment Framework for Selected Italian Airports: A Focus on Extreme Temperature Events". In: *Climate Services* 30 (Apr. 1, 2023), p. 100390. ISSN: 2405-8807. DOI: 10.1016/j.cliser.2023.100390. URL: https://www.sciencedirect.com/science/article/pii/S2405880723000511 (visited on 04/07/2024).

[18] Carmela De Vivo et al. "Climate-Risk Assessment Framework for Airports under Extreme Precipitation Events: Application to Selected Italian Case Studies". In: *Sustainability* 15.9 (9 Jan. 2023), p. 7300. ISSN: 2071-1050. DOI: 10.3390/su15097300. URL: https://www.mdpi.com/2071-1050/15/9/7300 (visited on 04/07/2024).

[19] Carmela De Vivo et al. "Risk Assessment Framework for Mediterranean Airports: A Focus on Extreme Temperatures and Precipitations and Sea Level Rise". In: *Natural Hazards* 111.1 (Mar. 1, 2022), pp. 547–566. ISSN: 1573-0840. DOI: 10.1007/s11069-021-05066-0. URL: https://doi.org/10.1007/s11069-021-05066-0 (visited on 04/07/2024).

[20] Angela Dean et al., eds. *Handbook of Design and Analysis of Experiments*. New York: Chapman and Hall/CRC, June 26, 2015. 960 pp. ISBN: 978-0-429-09634-1. DOI: 10.1201/b18619.

[21] Francisco J. Doblas-Reyes et al. "Linking Global to Regional Climate Change". In: *Climate Change 2021: The Physical Science Basis. Contribution of Working Group I to the Sixth Assessment Report of the Intergovernmental Panel on Climate Change*. Ed. by Valérie Masson-Delmotte et al. Cambridge, United Kingdom and New York, NY, USA: Cambridge University Press, 2021, pp. 1363–1512. DOI: 10.1017/9781009157896.001.

[22] Ralf Döscher et al. "The EC-Earth3 Earth System Model for the Coupled Model Intercomparison Project 6". In: *Geoscientific Model Development* 15.7 (Apr. 8, 2022), pp. 2973–3020. ISSN: 1991-959X. DOI: 10.5194/gmd-15-2973-2022. URL: https://gmd.copernicus.org/articles/15/2973/2022/ (visited on 09/14/2024).

[23] U. Ehret et al. "HESS Opinions "Should We Apply Bias Correction to Global and Regional Climate Model Data?"". In: *Hydrology and Earth System Sciences* 16.9 (Sept. 21, 2012), pp. 3391–3404. ISSN: 1027-5606. DOI: 10.5194/hess-16-3391-2012. URL: https://hess.copernicus.org/articles/16/3391/2012/ (visited on 09/15/2024).

[24] ENAC. *Torino Caselle - Aeroporti strumentali*. ENAC, 2014. URL: https://www.enac.gov.it/node/35361/ (visited on 09/26/2024).

[25] *ETCCDI Climate Change Indices*. URL: http://etccdi.pacificclimate.org/list_27_indices.shtml (visited on 03/18/2024).

[26] *European Climate Risk Assessment*. Publication. European Environment Agency, Jan. 2024. URL: https://www.eea.europa.eu/publications/european-climate-risk-assessment (visited on 04/09/2024).

[27] Veronika Eyring et al. "Overview of the Coupled Model Intercomparison Project Phase 6 (CMIP6) Experimental Design and Organization". In: *Geoscientific Model Development* 9.5 (May 26, 2016), pp. 1937–1958. ISSN: 1991-959X. DOI: 10.5194/gmd-9-1937-2016. URL: https://gmd.copernicus.org/articles/9/1937/2016/ (visited on 09/09/2024).

[28] James H. Faghmous and Vipin Kumar. "A Big Data Guide to Understanding Climate Change: The Case for Theory-Guided Data Science". In: *Big Data* 2.3 (Sept. 2014), pp. 155–163. ISSN: 2167-6461. DOI: 10.1089/big.2014.0026. URL: https://www.liebertpub.com/doi/10.1089/big.2014.0026 (visited on 08/11/2024).

[29] Christopher B. Field et al., eds. *Managing the Risks of Extreme Events and Disasters to Advance Climate Change Adaptation: Special Report of the Intergovernmental Panel on Climate Change*. Cambridge: Cambridge University Press, 2012. ISBN: 978-1-139-17724-5. DOI: 10.1017/CBO9781139177245. URL: http://ebooks.cambridge.org/ref/id/CBO9781139177245 (visited on 03/21/2024).

[30] GIZ. *Risk Supplement to the Vulnerability Sourcebook Guidance on How to Apply the Vulnerability Sourcebook's Approach with the New IPCC AR5 Concept of Climate Risk*. 2017. URL: https://climate-adapt.eea.europa.eu/en/metadata/guidances/risk-supplement-to-the-vulnerability-sourcebook-guidance-on-how-to-apply-the-vulnerability-sourcebook2019s-approach-with-the-new-ipcc-ar5-concept-of-climate-risk (visited on 06/09/2024).

[31] GIZ. *Vulnerability Sourcebook Annex - Adaptation Community*. Mar. 24, 2017. URL: https://www.adaptationcommunity.net/publications/vulnerability-sourcebook-annex/ (visited on 06/10/2024).

[32] José Manuel Gutiérrez et al. "Annex VI: Climatic Impact-Driver and Extreme Indices". In: *Climate Change 2021: The Physical Science Basis. Contribution of Working Group I to the Sixth Assessment Report of the Intergovernmental Panel on Climate Change*. Ed. by Valérie Masson-Delmotte et al. Cambridge, United Kingdom and New York, NY, USA: Cambridge University Press, 2021, pp. 2205–2214. DOI: 10.1017/9781009157896.001.

[33] Linda I. Hain, Julian F. Kölbel, and Markus Leippold. "Let's Get Physical: Comparing Metrics of Physical Climate Risk". In: *Finance Research Letters* 46 (May 1, 2022), p. 102406. ISSN: 1544-6123. DOI: 10.1016/j.frl.2021.102406. URL: https://www.sciencedirect.com/science/article/pii/S1544612321004013 (visited on 04/22/2024).

[34] A. Hannachi, I. T. Jolliffe, and D. B. Stephenson. "Empirical Orthogonal Functions and Related Techniques in Atmospheric Science: A Review". In: *International Journal of Climatology* 27.9 (2007), pp. 1119–1152. ISSN: 1097-0088. DOI: 10.1002/joc.1499. URL: https://onlinelibrary.wiley.com/doi/abs/10.1002/joc.1499 (visited on 08/29/2024).

[35] H. Hersbach et al. *ERA5 Hourly Data on Single Levels from 1940 to Present*. Copernicus Climate Change Service (C3S) Climate Data Store (CDS), 2023. DOI: 10.24381/CDS.ADBB2D47. URL: https://cds.climate.copernicus.eu/doi/10.24381/cds.adbb2d47 (visited on 04/16/2024).

[36] Hans Hersbach et al. "The ERA5 Global Reanalysis". In: *Quarterly Journal of the Royal Meteorological Society* 146.730 (2020), pp. 1999–2049. ISSN: 1477-870X. DOI: 10.1002/qj.3803. URL: https://onlinelibrary.wiley.com/doi/abs/10.1002/qj.3803 (visited on 06/30/2024).

[37] Chris Hewitt, Simon Mason, and David Walland. "The Global Framework for Climate Services". In: *Nature Climate Change* 2.12 (Dec. 2012), pp. 831–832. ISSN: 1758-6798. DOI: 10.1038/nclimate1745. URL: https://www.nature.com/articles/nclimate1745 (visited on 09/09/2024).

[38] ICAO. *Climate Adaptation Synthesis*. 2018. URL: https://www.icao.int/environmental-protection/Pages/Climate-Adaptation.aspx (visited on 09/23/2024).

[39] ICAO. *ICAO Environmental Report 2022*. 2022. URL: https://www.icao.int/environmental-protection/Pages/envrep2022.aspx (visited on 09/23/2024).

[40] IPCC. *Climate Change 2022: Impacts, Adaptation and Vulnerability. Working Group II Contribution to the Sixth Assessment Report of the Intergovernmental Panel on Climate Change*. Ed. by Hans-Otto Pörtner et al. Cambridge, United Kingdom and New York, NY, USA: Cambridge University Press, 2022. 3056 pp. ISBN: 978-1-00-932584-4. DOI: 10.1017/9781009325844. URL: https://www.cambridge.org/core/books/climate-change-2022-impacts-adaptation-and-vulnerability/161F238F406D530891AAAE1FC76651BD (visited on 04/23/2024).

[41] *ISO 14091:2021*. URL: https://www.iso.org/standard/68508.html (visited on 04/06/2024).

[42] Claus Kondrup et al., eds. *Climate Adaptation Modelling*. Springer Climate. Cham: Springer International Publishing, 2022. ISBN: 978-3-030-86211-4. DOI: 10.1007/978-3-030-86211-4. URL: https://link.springer.com/10.1007/978-3-030-86211-4 (visited on 09/04/2024).

[43] Lilian Loyer et al. *Inventory of Data Tools and Knowledge for Climate Impacts, Extremes and Risks for the Formulation of Standards That Can Increase Their Quality and Usefulness*. D2.5 of the Climateurope project. 2024. URL: https://climateurope2.eu/resources/public-deliverables (visited on 09/09/2024).

[44] J. B. Robin Matthews et al. "Annex VII: Glossary". In: *Climate Change 2021: The Physical Science Basis. Contribution of Working Group I to the Sixth Assessment Report of the Intergovernmental Panel on Climate Change*. Ed. by Valérie Masson-Delmotte et al. Cambridge, United Kingdom and New York, NY, USA: Cambridge University Press, 2021, pp. 2215–2256. DOI: 10.1017/9781009157896.001.

[45] Adam H. Monahan et al. "Empirical Orthogonal Functions: The Medium Is the Message". In: (Dec. 15, 2009). DOI: 10.1175/2009JCLI3062.1. URL: https://journals.ametsoc.org/view/journals/clim/22/24/2009jcli3062.1.xml (visited on 06/20/2024).

[46] Majid Niazkar et al. "Bias Correction of ERA5-Land Temperature Data Using Standalone and Ensemble Machine Learning Models: A Case of Northern Italy". In: *Journal of Water and Climate Change* 15.1 (Dec. 29, 2023), pp. 271–283. ISSN: 2040-2244. DOI: 10.2166/wcc.2023.669. URL: https://doi.org/10.2166/wcc.2023.669 (visited on 06/22/2024).

[47] Brian C. O'Neill et al. "The Roads Ahead: Narratives for Shared Socioeconomic Pathways Describing World Futures in the 21st Century". In: *Global Environmental Change* 42 (Jan. 1, 2017), pp. 169–180. ISSN: 0959-3780. DOI: 10.1016/j.gloenvcha.2015.01.004. URL: https://www.sciencedirect.com/science/article/pii/S0959378015000060 (visited on 09/09/2024).

[48] OECD. *Handbook on Constructing Composite Indicators: Methodology and User Guide*. Paris: Organisation for Economic Co-operation and Development, 2008. URL: https://www.oecd-ilibrary.org/economics/handbook-on-constructing-composite-indicators-methodology-and-user-guide_9789264043466-en (visited on 07/01/2024).

[49] C. Piani et al. "Statistical Bias Correction of Global Simulated Daily Precipitation and Temperature for the Application of Hydrological Models". In: *Journal of Hydrology* 395.3 (Dec. 15, 2010), pp. 199–215. ISSN: 0022-1694. DOI: 10.1016/j.jhydrol.2010.10.024. URL: https://www.sciencedirect.com/science/article/pii/S0022169410006475 (visited on 07/22/2024).

[50] Hans-Otto Pörtner et al. "Technical Summary". In: *Climate Change 2022: Impacts, Adaptation and Vulnerability. Contribution of Working Group II to the Sixth Assessment Report of the Intergovernmental Panel on Climate Change*. Ed. by Hans-Otto Pörtner et al. Cambridge University Press, 2022.

[51] Luigi Puddu et al. *Corporate Social Responsibility Report 2014*. SAGAT Group, June 2015. URL: https://www.aeroportoditorino.it/en/sagat/group/company/corporate-responsibility (visited on 09/25/2024).

[52] Roshanka Ranasinghe et al. "Climate Change Information for Regional Impact and for Risk Assessment". In: *Climate Change 2021: The Physical Science Basis. Contribution of Working Group I to the Sixth Assessment Report of the Intergovernmental Panel on Climate Change*. Ed. by Valérie Masson-Delmotte et al. Cambridge, United Kingdom and New York, NY, USA: Cambridge University Press, 2021, pp. 1767–1926. DOI: 10.1017/9781009157896.001.

[53] Andy Reisinger, Mark Howden, and Carolina Vera. *The Concept of Risk in the IPCC Sixth Assessment Report: A Summary of Cross-Working Group Discussions*. Geneva, Switzerland: Intergovernmental Panel on Climate Change, 2020, p. 15.

[54] Andrea Saltelli et al. "Why so Many Published Sensitivity Analyses Are False: A Systematic Review of Sensitivity Analysis Practices". In: *Environmental Modelling & Software* 114 (Apr. 1, 2019), pp. 29–39. ISSN: 1364-8152. DOI: 10.1016/j.envsoft.2019.01.012. URL: https://www.sciencedirect.com/science/article/pii/S1364815218302822 (visited on 06/27/2024).

[55] UN Secretary-General. *Report of the Open-ended Intergovernmental Expert Working Group on Indicators and Terminology Relating to Disaster Risk Reduction*. UN, Dec. 1, 2016. URL: https://digitallibrary.un.org/record/852089 (visited on 09/04/2024).

[56] Sonia I. Seneviratne et al. "Weather and Climate Extreme Events in a Changing Climate". In: *Climate Change 2021: The Physical Science Basis. Contribution of Working Group I to the Sixth Assessment Report of the Intergovernmental Panel on Climate Change*. Ed. by Valérie Masson-Delmotte et al. Cambridge, United Kingdom and New York,

NY, USA: Cambridge University Press, 2021, pp. 1513–1766. DOI: 10.1017/9781009157896.001.

[57] Nicholas P. Simpson et al. "A Framework for Complex Climate Change Risk Assessment". In: *One Earth* 4.4 (Apr. 23, 2021), pp. 489–501. ISSN: 2590-3322. DOI: 10.1016/j.oneear.2021.03.005. URL: https://www.sciencedirect.com/science/article/pii/S2590332221001792 (visited on 03/12/2024).

[58] *The 2023 Climate Risk Landscape: Technical Supplement*. URL: https://www.unepfi.org/themes/climate-change/2023-climate-risk-landscape-technical-supplement/ (visited on 04/09/2024).

[59] *The Vulnerability Sourcebook - Concept and Guidelines for Standardized Vulnerability Assessments — Discover the Key Services, Thematic Features and Tools of Climate-ADAPT*. URL: https://climate-adapt.eea.europa.eu/en/metadata/guidances/the-vulnerability-sourcebook-concept-and-guidelines-for-standardized-vulnerability-assessments (visited on 04/08/2024).

[60] B. Thrasher et al. "Technical Note: Bias Correcting Climate Model Simulated Daily Temperature Extremes with Quantile Mapping". In: *Hydrology and Earth System Sciences* 16.9 (Sept. 17, 2012), pp. 3309–3314. ISSN: 1027-5606. DOI: 10.5194/hess-16-3309-2012. URL: https://hess.copernicus.org/articles/16/3309/2012/hess-16-3309-2012.html (visited on 07/13/2024).

[61] Bridget Thrasher et al. "NASA Global Daily Downscaled Projections, CMIP6". In: *Scientific Data* 9.1 (June 2, 2022), p. 262. ISSN: 2052-4463. DOI: 10.1038/s41597-022-01393-4. URL: https://www.nature.com/articles/s41597-022-01393-4 (visited on 07/03/2024).

[62] Bridget Thrasher et al. *NEX-GDDP-CMIP6*. NASA Center for Climate Simulation, 2021. DOI: 10.7917/OFSG3345. URL: https://www.nccs.nasa.gov/services/data-collections/land-based-products/nex-gddp-cmip6 (visited on 05/02/2024).

[63] UNDRR. *Global Assessment Report on Disaster Risk Reduction 2019*. Geneva, Switzerland: United Nations Office for Disaster Risk Reduction (UNDRR), 2019. ISBN: 978-92-1-004180-5. URL: https://www.undrr.org/publication/global-assessment-report-disaster-risk-reduction-2019 (visited on 09/04/2024).

[64] Daniel S. Wilks. *Statistical Methods in the Atmospheric Sciences*. 4th ed. Elsevier, June 9, 2019. ISBN: 978-0-12-815823-4. URL: https://shop.elsevier.com/books/statistical-methods-in-the-atmospheric-sciences/wilks/978-0-12-815823-4 (visited on 08/29/2024).

[65] One Works, KPMG Advisory, and Nomisma. *Atlante degli aeroporti italiani*. ENAC, Sept. 2010. URL: https://www.enac.gov.it/pubblicazioni/studio-sugli-aeroporti-nazionali/studio-sullo-sviluppo-degli-aeroporti-italiani/ (visited on 09/16/2024).

Definitions

adaptation *process of adjustment to actual or expected climate (3.4) and its effects*, from [41]. 4

adaptive capacity *ability of systems (3.3), institutions, humans, and other organisms to adjust to potential damage, to take advantage of opportunities, or to respond to consequences*, from [41]. 4

anomaly *the deviation of a variable from its value averaged over a reference period*, from [44, p. 2218]. 10

average *the mean of monthly values of climatological data over any specified period of time (not necessarily starting in a year ending with the digit 1). In some sources, this is also referred to as provisional normal*, from [3, p. 2]. 10

climate service *climate services involve the provision of climate information in such a way as to assist decision-making. The service includes appropriate engagement from users and providers, is based on scientifically credible information and expertise, has an effective access mechanism and responds to user needs*, from [44, p. 2223] and [37, p. 831]. 2

climatological standard normal *averages of climatological data computed for the following consecutive periods of 30 years: 1 January 1981-31 December 2010, 1 January 1991-31 December 2020, and so forth*, from [3, p. 2]. *see* average

data assimilation *mathematical method used to combine different sources of information in order to produce the best possible estimate of the state of a system. This information usually consists of observations of the system and a numerical model of the system evolution. Data assimilation techniques are used to create initial conditions for weather forecast models and to construct reanalyses describing the trajectory of the climate system over the time period covered by the observations*, from [44, p. 2225]. *see* reanalysis, 13

determinant any component of risk, i.e. hazard, exposure, vulnerability, response, from [57, p. 493]. 3

driver individual component of a determinant, from [57, p. 493]. *see* determinant, hazard, vulnerability, exposure & response, 4

drought *an exceptional period of water shortage for existing ecosystems and the human population (due to low rainfall, high temperature, and/or wind)*, from [44, p. 2226]. 5

exposure *presence of people, livelihoods, species or ecosystems, environmental functions, services, resources, infrastructure, or economic, social or cultural assets in places and settings that could be affected*, from [41]. 3

hazard *potential source of harm*, from [41]. 3

heat wave *a period of abnormally hot weather, often defined with reference to a relative temperature threshold, lasting from two days to months. [...]*, from [44, p. 2233]. 19

heavy precipitation *an extreme/heavy precipitation event is an event that is of very high magnitude with a very rare occurrence at a particular place. [...]*, from [44, p. 2229]. 19

impact *effect on natural and human systems (3.3)*, from [41]. 3

impact chain *analytical approach that enables understanding of how given hazards (3.8) generate direct and indirect impacts (3.14) which propagate through a system (3.3) at risk (3.13)*, from [41]. *see* hazard, impact & risk, 18

indicator *quantitative, qualitative or binary variable that can be measured or described, in response to a defined criterion*, from [41]. 4

maladaptation *actions that may lead to increased risk of adverse climate-related outcomes, including via increased greenhouse gas (GHG) emissions, increased vulnerability to climate change, or diminished welfare, now or in the future. Maladaptation is usually an unintended consequence*, from [44, p. 2238]. 6

normal *period averages computed for a uniform and relatively long period comprising at least three consecutive ten-year periods*, from [3, p. 2]. *see* period average, 8

period average *averages of climatological data computed for any period of at least ten years starting on 1 January of a year ending with the digit 1*, from [3, p. 2]. *see* average, 10

reanalysis *reanalyses are created by processing past meteorological or oceanographic data using fixed state-of-the-art weather forecasting or ocean circulation models with data assimilation techniques. They are used to provide estimates of variables such as historical atmospheric temperature and wind or oceanographic temperature and currents, and other quantities. Using fixed data assimilation avoids effects from the changing analysis system that occur in operational analyses. Although continuity is improved, global reanalyses still suffer from changing coverage and biases in the observing systems*, from [44, p. 2245]. *see* data assimilation, 13

response action enact to mitigate the effects of climate change or adapt to it. 3

risk *effect of uncertainty*, from [41]. 1

risk management *coordinated activities to direct and control an organization with regard to risk (3.1)*, from [5]. *see* risk assessment, 1

risk assessment *the qualitative and/or quantitative scientific estimation of risks*, from [44, p. 2246]. *see* risk management, 1

sensitivity *degree to which a system (3.3) or species is affected, either adversely or beneficially, by climate (3.4) variability or change*, from [41]. 4

vulnerability *propensity or predisposition to be adversely affected*, from [41]. *see* sensitivity & adaptive capacity, 3

Acronyms

AR6 Sixth Assessment Report.

BA bias adjustment.

CCRA climate change risk assessment.

CDF cumulative distribution function.

CID climatic impact-driver.

CMIP6 Coupled Model Intercomparison Project Phase 6.

DRR disaster risk reduction.

ECMWF European Centre for Medium-Range Weather Forecasts.

ECV essential climate variable.

ENAC Ente Nazionale per l'Aviazione Civile.

EOF empirical orthogonal function.

ESM Earth system model.

GCM general circulation model.

ICAO International Civil Aviation Organization.

IPCC Intergovernmental Panel on Climate Change.

ISO International Organization for Standardization.

MIP Model Intercomparison Project.

ML Machine Learning.

NEX NASA Earth Exchange.

PC principal component.

QDM Quantile Delta Mapping.

QF quantile function.

QM Quantile Mapping.

SA sensitivity analysis.

SSP Shared Socioeconomic Pathway.

UA uncertainty analysis.

WMO World Meteorological Organization.

Symbols

$\diamondsuit$ placeholder for arbitrary argument or mathematical object.

$|\diamondsuit|$ absolute value or, if the argument is a set, cardinality.

$\mathbb{I}[\diamondsuit]$ symbolic representation of a conditional test: returns 1 if the condition in square brackets is satisfied, else 0 (i.e. generalisation of a characteristic function of the argument in square brackets).

DTR Diurnal Temperature Range.

tasmax Maximum Near-Surface Air Temperature.

tasmin Minimum Near-Surface Air Temperature.

tas Near-Surface Air Temperature.

$\diamondsuit|_{\mathbf{period}}$ relate the argument to the specified period.

pr Precipitation.